

# XLPR MODELS SUBGROUP REPORT

LEAK RATE



**PROBABILISTIC FRACTURE MECHANICS CODE**

## **DISCLAIMER**

THIS PUBLICATION WAS PREPARED AS AN ACCOUNT OF WORK JOINTLY SPONSORED BY THE ELECTRIC POWER RESEARCH INSTITUTE (EPRI) AND AN AGENCY OF THE U.S. GOVERNMENT. NEITHER EPRI NOR THE U.S. GOVERNMENT NOR ANY AGENCY THEREOF, NOR ANY EMPLOYEE OF ANY OF THE FOREGOING, MAKES ANY WARRANTY, EXPRESSED OR IMPLIED, OR ASSUMES ANY LEGAL LIABILITY OR RESPONSIBILITY FOR ANY THIRD PARTY'S USE, OR THE RESULTS OF SUCH USE, OF ANY INFORMATION, APPARATUS, PRODUCT, OR PROCESS DISCLOSED IN THIS PUBLICATION, OR REPRESENTS THAT ITS USE BY SUCH THIRD PARTY COMPLIES WITH APPLICABLE LAW.

THIS PUBLICATION DOES NOT CONTAIN OR IMPLY LEGALLY BINDING REQUIREMENTS. NOR DOES THIS PUBLICATION ESTABLISH OR MODIFY ANY REGULATORY GUIDANCE OR POSITIONS OF THE U.S. NUCLEAR REGULATORY COMMISSION AND IS NOT BINDING ON THE COMMISSION.

<b>xLPR Models Subgroup Report</b> <b>Leak Rate</b>	
<b>xLPR-MSGR-LRM Version 1.1</b>	
<b>Author Signature</b>	<b>Date</b>
<u>Elizabeth Kurth</u> Elizabeth Kurth, Emc <sup>2</sup> Leak Rate Module Subgroup Lead	09/22/16*
<b>Reviewer Signatures</b>	<b>Date</b>
<u>Paul Williams</u> Paul Williams, Oak Ridge National Laboratory Leak Rate Subgroup, Computational Group	05/27/16
<b>Approver Signatures</b>	<b>Date</b>
<u>Marjorie Erickson</u> Marjorie Erickson, PEAI xLPR Model's Group Lead	05/27/16
<u>Craig Harrington</u> Craig Harrington, Electric Power Research Institute xLPR Code Development Co-Lead	06/07/16

\*Editorial change requires only author approval.

THE TECHNICAL CONTENTS OF THIS DOCUMENT WERE NOT PREPARED IN  
ACCORDANCE WITH THE XLPR SOFTWARE QUALITY ASSURANCE PLAN.

Revision History		
Version Number	Description of Changes	Issue Date
1.0	Initial Issue	6/20/2016
1.1	<p>Corrected inconsistency in defining whether inner or outer diameter values are used to determine leakage rate from leak rate tables (see xLPR-REQ-32).</p> <p>The U.S. Nuclear Regulatory Commission Office of Nuclear Regulatory Research's and the Electric Power Research Institute's xLPR Project Contacts approved an administrative update in 2021 to support public release of this document without incrementing the version number or issue date. The administrative updates included: (a) title changed from "Leak Rate Module Development for xLPR Version 2.0" to "xLPR Models Subgroup Report—Leak Rate" throughout the document, (b) cover and title pages updated accordingly, (c) disclaimer statement added, (d) notice regarding official document version records storage location during code development removed as it is no longer needed, and (e) statement that the document was not prepared in accordance with the xLPR Software Quality Assurance Plan added.</p>	9/22/2016

## **EXECUTIVE SUMMARY**

The Leak Rate Subgroup was responsible for providing guidance and software code for determining the leakage rate of fluid flow through a crack for a given crack size, pressure, temperature and cracking mechanism. These calculations are performed by solving for equations developed by Henry and Fauske to represent fluid flow through a long pipe in which vapor generation occurs resulting in two phase flow. In order to more accurately adapt these equations to fluid flow through a crack, modifications to the equations are made to account for pressure losses due to entrance effects, phasic acceleration, friction, flow path deviations, flow area changes and crack morphology effects. Due to the computational time required to perform such calculations, a preprocessing module was developed in which the leakage rate software code, LEAPOR, developed by Oak Ridge National Laboratory, is used to generate leak rate tables as a function of crack length and crack-opening displacement for bounding pressure and temperature combinations and for both fatigue and PWSCC cracking mechanisms. These tables assume that the crack opening area on the inner and outer diameter are the same, i.e. that the fluid flows through an idealized crack shape. Since this is not what occurs in reality, during runtime of the xLPR code, the inner diameter crack size is used as input to obtain a leakage rate from the appropriate leak rate table. If the fluid flow is in the tight crack, two-phase choked flow regime, a correction is applied by also obtaining the leak rate based on the outside diameter crack dimensions and averaging the two. The dominant source of uncertainty in the leakage rate calculations comes from the crack morphology parameters. This is due to the limited amount of data used to develop the morphology parameters. To account for this uncertainty, another correction factor is applied for low leak rates. The workflow required to go from the idealized crack size leakage rate to the final leakage rate is described in this report. The technical basis, assumptions made, as well as their predicted impact on both the leakage rate and the probability of rupture are explained and discussed in this report. The verification and validation procedures that the LEAPOR code underwent are summarized. Additionally, lessons learned and recommendations for the leakage module of future versions of the xLPR code are provided.

## TABLE OF CONTENTS

<b>EXECUTIVE SUMMARY .....</b>	<b>IV</b>
<b>TABLE OF CONTENTS .....</b>	<b>V</b>
<b>LIST OF FIGURES .....</b>	<b>VII</b>
<b>LIST OF TABLES.....</b>	<b>VIII</b>
<b>ACRONYMS / LIST OF SYMBOLS .....</b>	<b>IX</b>
<b>1. INTRODUCTION.....</b>	<b>1</b>
1.1 Subgroup Roles and Responsibilities .....	1
1.2 Subgroup objectives .....	1
1.3 Models under auspices of subgroup.....	1
<b>2. LEAKAGE RATE MODEL DESCRIPTIONS .....</b>	<b>2</b>
2.1 Model requirements for xLPR .....	2
2.2 Model Inputs .....	5
2.3 Model Assumptions .....	9
2.4 Model Development.....	12
2.4.1 Mass-Flux Equation – Conservation of Momentum.....	13
2.4.2 Calculation of the Volumetric Flow Rate from the Mass Flow Rate.....	15
2.4.3 Pressure Drop Constraint Equation.....	16
2.4.4 Shapes of Cross-Sectional Flow Area of Crack Channel .....	21
2.4.5 Transition Model.....	23
2.4.6 Orifice Flow Model.....	26
2.5 Solution Strategy .....	26
2.6 Thermodynamic Properties of Water .....	26
2.7 Numerical Approximation of Derivatives.....	27
2.8 Different Inner and Outer Diameter Crack-Opening Areas .....	27
2.8.1 Correction Method .....	27
2.9 Uncertainty.....	29
2.9.1 Discharge Coefficient .....	29
2.9.2 Crack Morphology Variables .....	30
<b>3. LEAKAGE RATE MODEL IMPLEMENTATION.....</b>	<b>33</b>
3.1 Implementation Structure.....	33
3.2 Implementation of Model Requirements .....	33
3.2.1 LEAPOR Code Development .....	33
3.2.2 SR-LRM-008 – For the standalone application (Use Case 1), develop a graphical user interface. This requirement can be delayed until time and resources become available for a future implementation.....	34
3.2.3 SR-LRM-009 – Develop a suite of internal unit tests that exercise all significant elements of the new application.....	34
3.2.4 Regime Definitions .....	34
3.2.5 Error Codes .....	35
3.2.6 Preprocessing Application .....	37
3.3 Description of Inputs .....	39
3.3.1 LEAPOR USE Case 2 (preprocessing mode) inputs.....	39
3.3.2 Leak Rate module runtime inputs.....	39
3.4 Module Verification and Validation .....	40

3.4.1	Unit Test Verification .....	40
3.4.2	Database Verification .....	42
3.4.3	Software Verification.....	42
3.4.4	Experimental Validation.....	44
3.4.5	Engineering Judgement Validation.....	45
3.5	Flow Diagram.....	46
<b>4.</b>	<b>RECOMMENDATIONS FOR XLPR VERSION 3 MODIFICATIONS.....</b>	<b>48</b>
<b>5.</b>	<b>LESSONS-LEARNED.....</b>	<b>49</b>
<b>6.</b>	<b>SUMMARY.....</b>	<b>50</b>
<b>7.</b>	<b>REFERENCES.....</b>	<b>51</b>

## LIST OF FIGURES

Figure 1.	Two-phase flow through a long narrow crack channel: (a) flow regimes and (b) modeled geometry of flow path.....	14
Figure 2.	Implementation of Darcy friction factor, $f$ , as a function of the ratio of the hydraulic diameter, $D_h$ , to the effective surface roughness, $\mu$ . ....	19
Figure 3.	Crack flow area shapes: (a) rectangle, (b) diamond and (c) ellipse.....	22
Figure 4.	(Fig. 4 from ref. 37 ) Plot of critical pressure ratio as a function of the ratio of the crack depth (i.e., pipe wall thickness, $L$ ) to hydraulic diameter, $D_h$ , showing when the leak rate models in SQUIRT are valid and when they are not. ....	23
Figure 5.	Transition Model – regime definitions (morphology model turned off). ....	24
Figure 6.	Transition Model – regimes mapped onto volumetric flow rate (morphology model turned on) .....	25
Figure 9.	Power law fit to the COV as a function of the mean leak rate for the four pressure temperature combinations .....	31
Figure 10.	Unit Test Percent Error of Calculated vs Expected Result (Percent Error vs Case Number) .....	41
Figure 11.	Database Inspection Utility Results .....	42
Figure 12.	Percent Error between LEAPOR and SQUIRT runs.....	43
Figure 13.	LEAPOR and SQUIRT predicted versus measured leak rates.....	44
Figure 14.	All Experimental Data up to 10 gpm (approximately 0.63 kg/s).....	45
Figure 15.	Calculated Leak Rates for two different COD values over all four regimes .....	46



## LIST OF TABLES

Table 1.	Description of Leakage Rate Software Code Input Variables for Preprocessing Model .....	6
Table 2.	Description of Leakage Rate Software Code Output for Preprocessing Mode.....	7
Table 3.	Description of Leakage Rate Module Input Variables.....	8
Table 4.	Description of Leakage Rate Module Output Variables .....	9
Table 5.	Input parameters for $C_D$ test cases .....	30
Table 6.	Maximum percent error for varying $C_D$ .....	30
Table 7.	LEAPOR Error Codes .....	36
Table 8.	Inputs Read by xLPR LEAPOR Preprocessing Application.....	37
Table 9.	Minimum and Maximum Pressure and Temperature for Leakage Rate Tables .....	38
Table 10.	Crack Morphology mean and standard deviation values .....	39

## ACRONYMS / LIST OF SYMBOLS

ASME	American Society of Mechanical Engineers
CFD	Computational Fluid Dynamics
COA	Crack-Opening Area
COD	Crack-Opening Displacement
COV	Coefficient of Variation
DLL	Dynamic Link Library
HEM	Homogeneous Equilibrium Model
LEAPOR	Leak Analysis of Piping – Oak Ridge
LRM	Leak Rate Module
MVR	Module Validation Report
NNES	Nonmonotonic Nonlinear Equation Solver
ORNL	Oak Ridge National Laboratory
PICEP	Pipe Crack Evaluation Program
PWSCC	Primary Water Stress Corrosion Cracking
SDD	Software Design Description
SQA	Software Quality Assurance
SQUIRT	Seepage Quantification of Upsets in Reactor Tubes
SRD	Software Requirements Document
STP	Software Test Plan
STRR	Software Test Results Report
xLPR	eXtremely Low Probabilty of Rupture

$A_0$	flow area at crack entrance plane
$A_c$	flow area at throat
$A_l$	flow area where vapor generation begins
$C_D$	discharge coefficient
$D_h$	hydraulic diameter
$e_{vloss}$	velocity head loss
$f$	Darcy friction factor
$G_c$	mass flux at crack exit plane
$K_G$	global flow path deviation from straight
$K_{G+L}$	local flow path deviation from straight
$L$	total length of the flow path
$L_{eff}$	effective length of the flow path
$\dot{m}$	mass flow rate
$N$	emperical parameter
$p_0$	absolute stagnation pressure at the crack entrance
$p_a$	pressure due to acceleration by vaporization
$p_{aa}$	pressure due to acceleration by changing flow area
$p_c$	absolute pressure at throat
$p_e$	pressure due to entrance effects
$p_f$	pressure due to frictional effects
$p_k$	pressure due to tortuosity of flow path
$P_w$	wetted perimeter

$Q$	volumetric flow rate
$v_{fg(c)}$	specific volume change due to vaporization at throat
$v_{g(c)}$	specific volume of saturated vapor at throat
$v_{l(0)}$	specific volume of subcooled liquid at crack entrance plane
$v_{std}$	specific volume at standard conditions
$X_c$	non-equilibrium vapor quality at throat
$X_{c(h)}$	isenthalpic equilibrium vapor quality at crack exit plane
$X_E$	equilibrium vapor quality at throat
$z$	distance along fluid flow path
$\delta_{COD}$	crack-opening displacement
$\gamma_0$	isentropic expansion coefficient for wet or superheated vapor
$\mu$	effective surface roughness
$\mu_G$	global surface roughness
$\mu_L$	local surface roughness
$\eta_t$	effective number of turns
$\eta_{tL}$	local number of turns

## 1. INTRODUCTION

### 1.1 Subgroup Roles and Responsibilities

The Leak Rate Module (LRM) Subgroup was responsible for identifying and developing all of the models incorporated into the xLPR computational framework to predict the leakage rate of fluid flow through a crack. The selected models are best-estimate, computationally efficient, widely accepted models that reliably represent available leakage rate data within the range of applicability established for the xLPR code. The subgroup incorporated the selected models into a computationally efficient module and provided clear descriptions and appropriate quantification of all sources of uncertainty in model parameters.

### 1.2 Subgroup objectives

The primary objectives of the LRM Subgroup are:

- Develop the software code to calculate leakage rates given the crack size parameters on the inner and outer diameter, and pipe operating conditions.
- Develop a preprocessing method to create leak rate tables that the framework can read and interpolate given the crack size parameters on the outer diameter and pipe operating conditions.
- Develop a method to correct for leakage rates when the crack size is not equal on the inner and outer diameter.
- Define the necessary test cases for use in verifying and validating leakage rate calculations.
- Characterize model parameter and input value uncertainty.
- Produce leak rate model documentation.

### 1.3 Models under auspices of subgroup

The Leak Rate Subgroup determined which models would be used in the calculation of fluid flow through a crack. This includes models for the fluid thermohydraulic process, the loss of pressure due to crack properties, crack opening shape models, and the effect on leakage rates due to crack morphology parameters. The crack-opening displacements, crack lengths, and leak detection are addressed by other xLPR subgroups.

A software code, **Leak Analysis of Piping – Oak Ridge** (LEAPOR) [27] was written at Oak Ridge National Laboratory (ORNL) to calculate the leakage rates for given crack sizes, pipe geometry and operating conditions. The thermohydraulic model implemented into LEAPOR has been used in other leakage rate codes including PR-LEAK, **Pipe Crack Evaluation Program** (PICEP) and **Seepage Quantification of Upsets In Reactor Tubes** (SQUIRT) and is generally regarded as providing a good estimate of flow rates through long cylinders. In order to more accurately model flow through a crack, rather than a long cylinder, pressure loss terms are introduced that address pressure reduction due to entrance losses, friction, acceleration, flow area changes, and path tortuosity. Additionally, the crack opening shape is modeled as an ellipse to more realistically model the crack shape. These models are described in detail in Section 2.4.

Due to computational limitations of the Framework the LEAPOR code is run as a preprocessor outputting leak rate tables for either Primary Water Stress Corrosion Cracking (PWSCC), fatigue or both cracking mechanisms acting together as functions of crack-opening area, crack length, pressure and temperature. The Framework uses these tables during runtime and interpolates to find the correct leakage rate based on the inner diameter crack opening area. If the inner diameter crack opening area (COA) is not the same as the outer diameter area modifications to the leakage rate found in the table are made. The modification is using the average of the leak rate calculated using the inner diameter crack length and COD and the leak rate calculated using the outer diameter crack length and COD. This method is described in detail in Section 2.8.

The main source of uncertainty for the Leak Rate module is due to the crack morphology parameters. The crack morphology parameters were developed to better represent the fluid path through a crack in a pipe, and are therefore dependent on the cracking mechanism, i.e. fatigue or stress corrosion. The data from which the crack morphology parameters were developed is very limited. The inability to accurately validate these parameters to real cracks is the primary contributor to this uncertainty. It is recommended that more crack morphology measurements are performed on cracks found in service. In the meantime, the uncertainty in these parameters is accounted for by applying a modification to the leak rate value when it is below 10 gpm. This method is described in Section 2.9.

## **2. LEAKAGE RATE MODEL DESCRIPTIONS**

The leak rate calculations are carried out during pre-processing operations and stored in leak rate tables as a function of crack-opening displacement (COD), crack length, cracking mechanism, pressure, and temperature. During runtime the Framework interpolates between the appropriate tables based on user input of the pressure and temperature and the calculated crack size by the xLPR code. If necessary, the Framework then applies modifications to this leak rate to account for different crack-opening area (COA) values on the inner and outer diameter and uncertainty due to the crack morphology parameters.

### **2.1 Model requirements for xLPR**

This section contains the specific requirements for the design of the software code LEAPOR and the implementation of LEAPOR into the xLPR code. The LEAPOR leak-rate service is exposed via a Dynamic Link Library (DLL) to the xLPR Framework during the preprocessing stage through the inputs spreadsheet and Excel preprocessor plug-in. The following list describes the functional requirements of the Leak Rate Module [51]

- **SR-LRM-001** – Develop a software application that will calculate an estimate for the leakage rate of water escaping from a postulated through-wall crack in a piping segment of a nuclear power plant cooling water system.
- **SR-LRM-002** – Implement the extended Henry-Fauske thermohydraulic model [16-18] that is used in the SQUIRT code [40] for tight cracks.
- **SR-LRM-003** – The new application must be designed in such a way that the design attributes of maintainability, portability, and extensibility can be realized successfully by future developers who were not necessarily involved in the original task of creating the software.

- **SR-LRM-004** – The new application must comply with all xLPR Project Software Quality Assurance (SQA) requirements including evaluations for correctness, consistency, completeness, accuracy, readability, and testability, and be prepared to successfully meet the criteria of all SQA audits.
- **SR-LRM-005** – Develop the Leakage Rate Module for two general use cases<sup>1</sup> :
  - **Use Case 1:** a standalone code with a human actor using a console application run from a blind prompt window, and
  - **Use Case 2:** an external DLL element where the actor is the GoldSim xLPR application or the preprocessor Excel Add-In application to be developed for the xLPR Excel Inputs Database. The same DLL shall be addressable by either actor. The Leakage Rate Module shall be embedded within DLL wrapper coding to be developed by the Computational Group.
- **SR-LRM-006** – The required inputs and outputs are presented in Table 1 -

---

<sup>1</sup> A *use case* is a list of steps or mode of operation, typically defining interactions between a role (known in the Unified Modeling Language (UML) as an “actor”) and a system, to achieve a specified goal. The actor can be a human or an external system or application.

- Table 4.
- **SR-LRM-007** – Internally, the physical models will be implemented using the SI system of units. When required, all unit conversions will be based on IEEE/ASTM SI 10™ 2010, *American National Standard for Metric Practice* [19].
- **SR-LRM-008** – For the standalone application (Use Case 1), develop a graphical user interface. This requirement can be delayed until time and resources become available for a future implementation.
- **SR-LRM-009** – Develop a suite of internal unit tests that exercise all significant elements of the new application.
- **SR-LRM-010** – Check for orifice-flow conditions and implement an appropriate model to handle this flow regime.
- **SR-LRM-011** – Develop a linear interpolation scheme within the new application to model the transition between orifice flow and flow through a tight crack.
- **SR-LRM-012** – Implement validity checks for all inputs and report invalid inputs to the user by returning a termination code flag.
- **SR-LRM-013** – Identify those conditions where the implemented models are not physically valid and report these cases to the user by returning a termination code flag.
- **SR-LRM-014** – For the preprocessing application (Use Case 2) generate leak rate tables for each cracking mechanism selected by the user (fatigue, PWSCC or both) for the input combinations of minimum pressure/minimum temperature, minimum pressure/maximum temperature, maximum pressure/minimum temperature and maximum pressure/maximum temperature.
- **SR-LRM-015** – For the preprocessing application (Use Case 2) provide default values for the minimum and maximum pressure and temperature values to be used in generating the leakage rate tables. The user may also override these default presets by entering user-defined pressure and temperature ranges in “xLPR-2.0 Input Set.xlsx” inputs database on the “User Options” worksheet (cells E142-E145, inclusive). The implementation of these values is the responsibility of the xLPR Preprocessing Application [47].
- **SR-LRM-016** – For the preprocessing application (Use Case 2) automatically determine the range and discretization of the crack lengths and crack-opening displacements used to generate the leakage rate tables.
- **SR-LRM-017** – For the preprocessing application (Use Case 2) provide default, recommended values for the crack morphology parameters.
- **SR-LRM-018** – For the preprocessing application (Use Case 2) provide guidance on how to apply a correction in cases in which the crack opening area differs on the inner and outer diameter.

- **SR-LRM-019** – In applications in which both fatigue and PWSCC mechanisms are being considered, provide guidance on which crack morphology parameters to use in determining which leak rate table to use for the leakage calculation.
- **SR-LRM-020** – Provide guidance on application of the uncertainty due to crack morphology parameters.

All requirements listed above have been implemented as part of the xLPR Program with the exception of requirement SR-LRM-008 which states that a graphical user interface will be developed for Use Case 1 of the LEAPOR code. Since this GUI application is not a necessary feature its development will be delayed to a future date. Requirements SR-LRM-014 through SR-LRM-020 are apportioned in part to the Framework through use of the pre-processing application as described below.

- **SR-LRM-014** – The LEAPOR code is developed to accept inputs to generate leak rate tables as required by this requirement, however, the actual creation of the tables is performed by the xLPR Preprocessing Application [47].
- **SR-LRM-015** – The Leak Rate Module provides default values for the minimum and maximum pressure and temperature values to be used in generating the leakage rate tables. The user may also override these default presets by entering user-defined pressure and temperature ranges located in “xLPR-2.0 Input Set.xlsx” inputs database on the “User Options” worksheet (cells E142-E145, inclusive). The implementation of these values is the responsibility of the xLPR Preprocessing Application [47].
- **SR-LRM-016** – The Leak Rate Module provides guidance on how to automatically determine the range and discretization of the crack lengths and crack-opening displacements used to generate the leakage rate tables and the implementation of the discretization is performed by the xLPR Preprocessing Application [47].
- **SR-LRM-017** – The Leak Rate Module provides default values for the crack morphology parameters and the Framework is responsible for implementation of these inputs. The user may also override these default presets by entering user-defined morphology parameters located in “xLPR-2.0 Input Set.xlsx” inputs database on the “User Options” worksheet (cells E130-E139, inclusive). The Framework is responsible for the implementation of these inputs.
- **SR-LRM-018** – The Leak Rate Module supports a correction method and guidance on the implementation of this method was provided. The xLPR Framework implements the correction to the leakage rate.
- **SR-LRM-019** – The Leak Rate Module provides guidance on which crack morphology parameters to use when both fatigue and PWSCC cracking mechanisms are used in determining which leak rate table to use for the leakage calculation and the Framework is responsible for implementing that decision process
- **SR-LRM-020** – The Leak Rate Module provides guidance on the application of the uncertainty due to crack morphology parameters and the Framework is responsible for the implementation of the uncertainty on the leakage rate.



## **2.2 Model Inputs**

The inputs required for the LEAPOR code used in Use Case 2 are shown in Table 1 and the outputs in

Table 2. The inputs and outputs required for Use Case 1 are described in the Leak Rate Module SRD[51] however since this Use Case is not used as part of the xLPR program they are not repeated here.

**Table 1. Description of Leakage Rate Software Code Input Variables for Preprocessing Model**

Input Variable Name	Description	Units	Default Value	Limits / Comments
Pressure_max	Maximum fluid stagnation pressure in the pipe used to create look-up tables	[kPa]	15.913	
Pressure_min	Minimum fluid stagnation pressure in the pipe used to create look-up tables	[kPa]	14.824	
Temperature_max	Maximum fluid stagnation temperature in the pipe used to create look-up tables	[°C]	340	
Temperature_min	Minimum fluid stagnation temperature in the pipe used to create look-up tables	[°C]	280	
Pipe_Thickness	The wall thickness of the pipe containing the crack.	[mm]		0 < Thickness_in < Pipe_Radius_Outer
Pipe_Radius_Outer	outer radius of the pipe	[mm]		
mode_in	operation mode flag	[-]		= -1 preprocessor mode (no debug output created) = 0 (no debug output created) = 1 (debug output created) = 2 (run internal unit tests)
mu_L1	local surface roughness for STYPE1	[microns]	16.86	
mu_G1	global surface roughness for STYPE1	[microns]	113.9	
eta_tL1	number of turns per unit length of flow path for STYPE1	[m <sup>-1</sup> ]	5940	
K_G1	global pathway parameter for STYPE1	[-]	1.009	
K_G_L1	local pathway parameter for STYPE1	[-]	1.243	
Ninc_2c	number of intervals for crack length in leak rate table	[-]		The user is unable to change this value
Ninc_cod	number of intervals for crack opening displacement in leak rate table	[-]		The user is unable to change this value
mu_L2	local surface roughness for STYPE2	[microns]	8.814	
mu_G2	global surface roughness for STYPE2	[microns]	40.51	

Input Variable Name	Description	Units	Default Value	Limits / Comments
eta_tL2	number of turns per unit length of flow path for STYPE2	[m <sup>-1</sup> ]	6730	
K_G2	global pathway parameter for STYPE2	[-]	1.017	
K_G_L2	local pathway parameter for STYPE2	[-]	1.06	

**Table 2. Description of Leakage Rate Software Code Output for Preprocessing Mode**

Output Variable Name	Description	Units	Value	Limits / Comments
termcode	termination code	[-]		= 0 (solution found) != 0 (solution not found) See error codes in Table 7
runtime	cpu time	[sec]		
Ninc_2c	number of intervals for crack length in look-up table	[-]		
Ninc_cod	number of intervals for crack opening displacement in look-up table	[-]		
Crack_length_out	Ninc_2c discretization of crack lengths used in look-up table	[mm]		contained in array out(11 : N2-1) where N2=11+Ninc_2c
COD_out	Ninc_cod discretization of crack opening displacements used in look-up table	[mm]		contained in array out(N2 : N3-1) where N3=N2+Ninc_cod
LeakRate_PWSCC	Ninc_2c x Ninc_cod look-up table for PWSCC crack morphology	[gpm]		contained in array out(N3 : N4-1) where N4=N3+Ninc_2c*Ninc_cod
LeakRate_Fatigue	Ninc_2c x Ninc_cod look-up table for fatigue crack morphology	[gpm]		contained in array out(N4 : N5-1) where N5=N4+Ninc_2c*Ninc_cod

The inputs required by the Framework to determine the leakage rate and apply the corrections described by requirements SR-LRM-018 and SR-LRM-020 during runtime are shown in Table 3 and the outputs in

Table 4. The inner diameter crack length, inner diameter COD, thickness, pressure, temperature, and cracking mechanism are all inputs needed to determine the correct leak rate table(s) to use. For tight cracks with two-phase choked flow conditions (Regime 1 as defined in 2.4.5.1), the leakage rate is also determined using the outer diameter crack length and outer diameter COD. This leakage rate is then averaged with the inner diameter leak rate originally obtained from the tables. The final outputs from the Leak Rate module are the leakage rates (both mass and volumetric flow rates), and the correction factor due to uncertainty.

**Table 3. Description of Leakage Rate Module Input Variables**

Input Variable Name	Description	Units	Value	Limits / Comments
Crack_Length_Outer_in	Total crack length on the outer diameter (2c)	[mm]		$0 < \text{Crack\_Length\_Outer\_in} < \pi * \text{Pipe\_ID}$
COD_Outer_in	crack-opening displacement on the outer diameter	[mm]		$\text{COD\_Outer\_in} > 0$
Thickness_in	The wall thickness of the pipe containing the crack.	[mm]		$0 < \text{Thickness\_in} < \text{Pipe\_Radius\_Outer\_in}$
Temperature_in	Fluid stagnation temperature in the pipe	[°C]		
Pressure_in	Fluid stagnation pressure in the pipe	[kPa]		
STYPE	cracking mechanism	[-]		= 1 (IGSCC) = 2 (PWSCC Base) = 3 (PWSCC Weld) = 4 (Fatigue) = 5 (Other)
Crack_Length_Inner_in	Total crack length on the inner diameter (2c)	[mm]		$0 < \text{Crack\_Length\_Inner\_in} < \pi * \text{Pipe\_ID}$
COD_Inner_in	crack-opening displacement on the inner diameter	[mm]		$\text{COD\_Inner\_in} > 0$

**Table 4. Description of Leakage Rate Module Output Variables**

<b>Output Variable Name</b>	<b>Description</b>	<b>Units</b>	<b>Value</b>	<b>Limits / Comments</b>
ufactor	factor applied to account for uncertainty due to crack morphology	[-]		
LeakRate_out <sup>2</sup>	Volumetric Leakage Rate	[gpm]		see ISA-67.03-1982 [39]
LeakRate_mass_out	Mass Leakage Rate	[kg/s]		see ISA-67.03-1982 [39]

## 2.3 Model Assumptions

The assumptions made to support the Leak Rate model development are summarized here with potential implications on the resulting xLPR analysis.

<b>Assumption</b>	<b>Technical Support/ Reason for Assumption</b>	<b>Implication</b>
The flow is a steady state condition	References 16,17,18	None
The flow is adiabatic	References 16,17,18	None
The fluid at the crack entrance is a subcooled incompressible liquid	References 16,17,18	None
At a prescribed empirically-derived position along the flow path (12 times the hydraulic diameter, $D_h$ ), the metastable liquid initiates bubble nucleation and, thus, vapor generation	References 16,17,18	None
The fluid at the onset of vapor generation experiences an isentropic expansion	References 16,17,18	None
The liquid and vapor phases in the vapor-generation region of the model are in mechanical (phasic velocities are equal) and thermal equilibrium.	References 16,17,18	None

<sup>2</sup> The volumetric flow rate is calculated from the mass flow rate based on a water temperature of 20 °C (68 °F) and a pressure of 101.35 kPa (14.7 psia) as specified in ISA-67.03-1982 [39].

Assumption	Technical Support/ Reason for Assumption	Implication
The entire process of state changes from the crack entrance plane to the crack exit plane is assumed to be adiabatic and thermodynamically reversible, and therefore, isentropic, such that the entropy of the subcooled liquid water in the pipe is equal to the entropy of the equilibrium mixture of vapor and liquid phases at the crack exit plane	References 16,17,18	None
<p>The isentropic rate of vapor generation is reduced by exponentially relaxing the evolution of the vapor quality through the application of an empirically-derived coefficient, N. The non-equilibrium vapor quality at the throat, <math>x_c</math>, is modeled as:</p> $x_c = Nx_E \left\{ 1 - \exp \left[ -B \left( \frac{L}{D_h} - 12 \right) \right] \right\}$ <p>where <math>x_E</math> is the vapor quality at the throat, <math>B=0.0523</math> is an empirically-derived constant, <math>L</math> is the length of the flow path through the wall and <math>D_h</math> is the hydraulic diameter of the flow path and the empirical parameter <math>N</math> is defined as</p> $N = \begin{cases} 20x_E & \text{for } x_E < 0.05 \\ 1 & \text{for } x_E \geq 0.05 \end{cases}$	This empirical adjustment moves the model away from the thermal-equilibrium assumption towards a more physically realistic non-equilibrium model	Unknown
Zero slip, i.e. ., mechanical equilibrium with the two phasic velocities assumed equal	References 16,17,18	None
The flow reaches a choked state at the crack exit plane, also referred to as the throat or choking plane, which represents the maximum flow rate that can occur for a given set of operating conditions	References 16,17,18	None
The calculation of volumetric flow rate will use the specific volume of subcooled liquid water at 20°C (68°F) and 101.35 kPa (14.7 psia)	This is the standard based on Reference 34	Required by ISA-67.03-1982 [39].

Assumption	Technical Support/ Reason for Assumption	Implication
The value for $C_D$ is 0.95 representing rounded or smooth-edged entrances [4].	At small length scales typically associated with a tight crack, the edges of the entrance plane will appear rounded or smooth relative to the small length scales of the inner surface morphology of the crack channel near the entrance	Negligible, see Section 2.9.1
<p>For the condition when <math>L/D_h \geq 12</math>, where <math>D_h</math> is the hydraulic diameter evaluated at the exit plane, the frictional pressure drop is calculated by:</p> $\Delta p_f = \frac{G_c^2}{2} \left\{ 12f \left( \frac{A_c^2}{A_i A_o} \right) v_{l(0)} + f \left( \frac{L}{D_h} - 12 \right) \left( \frac{A_c}{A_i} \right) [\bar{v}_f + \bar{x}_{(h)} \bar{v}_{fg}] \right\}$ <p>When <math>L/D_h &lt; 12</math> then the frictional pressure drop is calculated by:</p> $\Delta p_f = \frac{G_c^2}{2} \left\{ 12f \left( \frac{A_c^2}{A_i A_o} \right) v_{l(0)} \right\}$	The different frictional losses are due to the assumption that when $L/D_h = 12$ , the fluid transitions from a single-phase fluid to a two-phase fluid	Unknown
<p>The Darcy friction factor, <math>f</math>, is calculated using the following equation</p> $f = \left[ C_1 \log_{10} \left( \frac{D_h}{\mu} \right) + C_2 \right]^{-2}$	LEAPOR has implemented this relationship based on its programming in SQUIRT. However, the technical basis documented in SQUIRT for the coefficients is lacking and therefore it is recommended that this be further validated in the future	Unknown
<p>The velocity head loss is defined as</p> $e_{vloss} = \eta_t \left( \frac{L_{eff}}{L} \right) L = \eta_t L_{eff}$	This equation was determined based on programming in SQUIRT, however this relationship has not been documented anywhere and therefore it is recommended that this be further validated in the future	Unknown



<b>Assumption</b>	<b>Technical Support/ Reason for Assumption</b>	<b>Implication</b>
The increment size for the crack length and COD used to generate the tables is hard-coded	In order to ensure that an adequate range of leakage rates is calculated for the leak rate tables the user is not able to specify the increment size at this time	None
The minimum and maximum values of pressure and temperature are used to generate the leak rate tables	The values chosen cover the range of problems of interest from the LBB database	If a user inputs a pressure and/or temperature outside the minimum/maximum defined values the accuracy of the final leakage rate is unknown since the correction method for different ID and OD COAs and correction factor for uncertainty were developed using the default range
Linear interpolation of leakage rates in leak rate tables	The incremental size of the crack lengths and CODs which make up the tables are small enough in which linear interpolation is accurate	None
The inner diameter crack length and COD are used when looking up leakage rates from the leak rate tables	The inner diameter crack length and COD is nearly the same as that for the actual leak rate when the flow is in regimes 2, 3 or 4	None
When the flow is in Regime 1 an average of the leakage rate from the leak rate tables using the inner diameter crack properties and using the outer diameter crack properties is used	The technical basis for this assumption is provided in the LRM SDD and Section 2.8 of this report	Slight over-prediction of the leak rate may result as seen in Figure 8.
The correction for uncertainty due to the crack morphology variables is applied only if the leakage rate is less than 10 gpm	The technical basis for this assumption is provided in the LRM SDD and Section 2.9 of this report	Under-prediction of the leak rate may result if the difference between the inner and outer crack-opening areas is very large

## 2.4 Model Development

A general overview of the model development is provided in this section, whereas detailed information can be found in the Leak Rate Module SDD [48]. The goal of the Leak Rate Module is to calculate the leakage rate of high-temperature, high-pressure water in a sub-cooled state that is “flashing” (adiabatic flow boiling) through a crack in a pipe. The model required by SR-LRM-002 for this baseline release of the Leak Rate module for xLPR is the empirically-adjusted

homogeneous equilibrium model (HEM) developed by Henry and Fauske [16-18] with extensions by Abdollahian [1] and Paul et al. [30]. The HEM approach considers the two-phase mixture to be a pseudo-fluid which can be described by the same conservation law principles that are valid for a single-phase flow condition [43]. For an adiabatic flow the process is assumed to be reversible and, therefore, isentropic, and the velocities of the two phases are assumed to be equal. The equilibrium properties of the two phases can be obtained from a water-property formulation (“Steam Tables”) implemented in code or from some general equation of state. Abdollahian [1] extended the Henry-Fauske non-equilibrium model by including additional terms for pressure losses due to entrance effects, acceleration by vaporization, acceleration by changing cross-sectional flow area, and frictional effects. At Battelle, Paul et al. [30] further extended the Henry-Fauske model by including pressure losses due to the tortuosity of the flow path resulting from turns and protrusions in the surface morphology of the two crack faces. The Battelle model is implemented (with some revisions that are identified in the LRM SDD) into the baseline version of the leak rate module. Sections 2.4.1 through 2.4.4 present the details of this model. Sections 2.4.5 and 2.4.6 describe the models used to calculate the leakage rate in those flow regimes that fall outside the Battelle model range of validity.

#### **2.4.1 Mass-Flux Equation – Conservation of Momentum**

The mass-flux equation is derived [16-18] from the one-dimensional conservation of momentum law and is further constrained by the conservation of mass. The details of this derivation are outlined in the Leak Rate Module SDD [48]. Figure 1 (taken from ref. 8) shows the two-phase flow regimes and the simplified geometry assumed for the model.

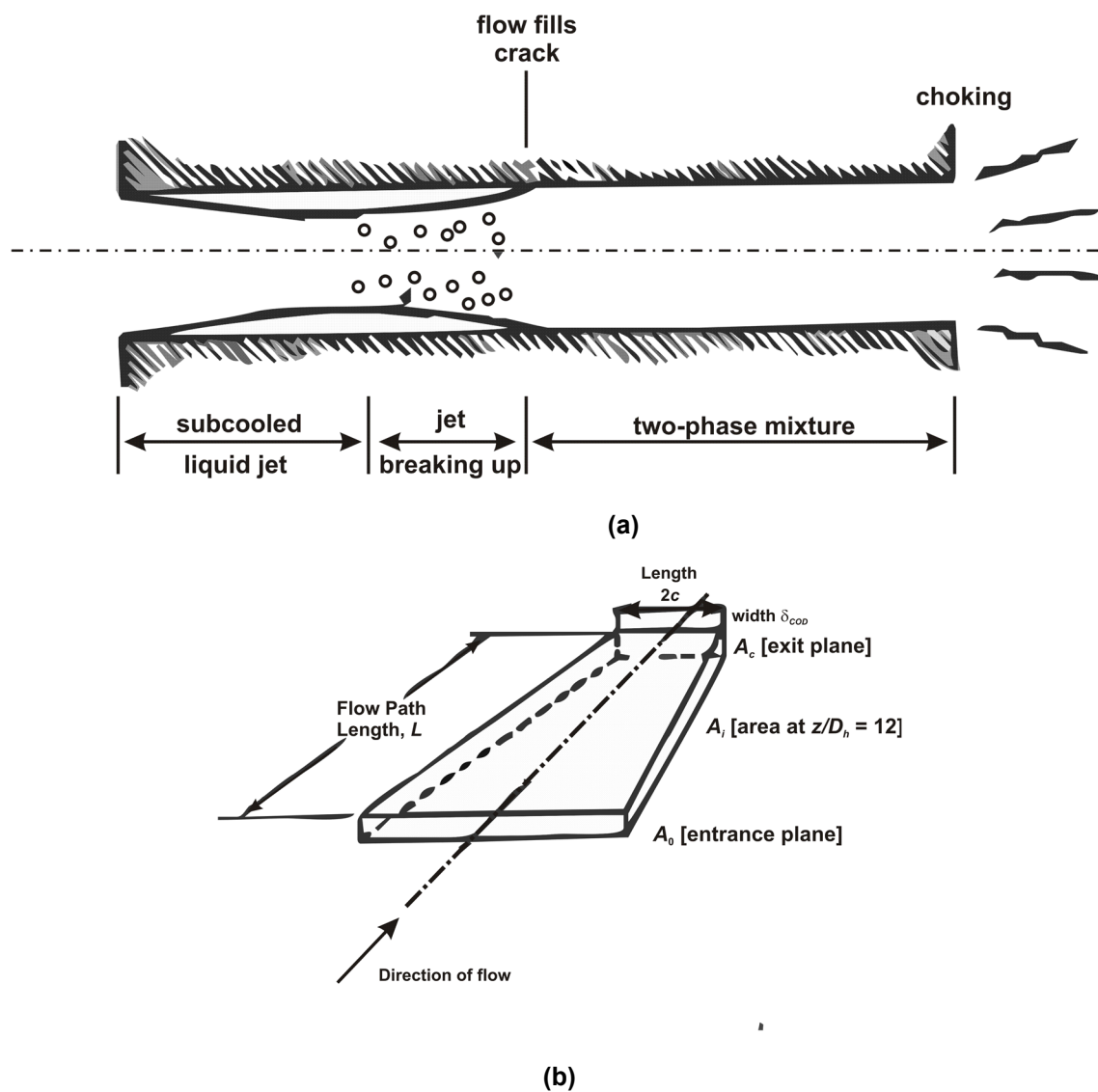


Figure 1. Two-phase flow through a long narrow crack channel: (a) flow regimes and (b) modeled geometry of flow path.

Equation 1 presents the mass-flux equation implemented in the code.

$$\psi(G_c^2, p_c) = G_c^2 - \frac{1}{\left[ \left( \frac{x_c v_{g(c)}}{\gamma_0 p_c} \right) - \left( v_{fg(c)} N \frac{dx_E}{dp_c} \right) \right]_c} = 0 \quad (\text{Equation 1})$$

where

$G_c$  = mass flux at crack exit plane (aka throat or choking plane) [kg/m<sup>2</sup>-sec]

$x_c$  = non-equilibrium vapor quality at throat [-]

$v_{g(c)}$  = specific volume of saturated vapor at throat [m<sup>3</sup>/kg]

$\gamma_0$  = isentropic expansion coefficient for wet or superheated vapor [-]

$p_c$  = absolute pressure at the throat [Pa] = [N/m<sup>2</sup>] = [kg/m-sec<sup>2</sup>]

$N$  = empirical parameter, see Eqs. (3)-(4).

$v_{fg(c)} = v_{g(c)} - v_{f(c)}$  = specific volume change due to vaporization evaluated at the throat [m<sup>3</sup>/kg]

$x_E$  = equilibrium vapor quality at the throat [-]

$\left. \frac{dx_E}{dp} \right|_c$  = first derivative of equilibrium vapor quality with respect to pressure at the throat [Pa]<sup>-1</sup> = [m<sup>2</sup>/N]

## 2.4.2 Calculation of the Volumetric Flow Rate from the Mass Flow Rate

Requirement SR-LRM-006 specifies that both the mass flow rate and the volumetric flow rate at the exit be among the outputs from the code. The volumetric flow rate,  $Q$ , can be calculated from the mass flow rate,  $\dot{m}$ , by

$$Q = \dot{m} v_{std} \quad (\text{Equation 2})$$

where  $v_{std}$  is the specific volume that satisfies the definition of the Leakage Rate. The standard ISA-67.03-1982 [41] (which is cited in Reg. Guide 1.45, rev. 1 [34]) defines the leakage rate as leakage expressed in volumetric units per unit of time at 20°C and one atmosphere pressure. Therefore, the calculation of volumetric flow rate will use the specific volume of subcooled liquid water at 20°C (68°F) and 101.35 kPa (14.7 psia).

### 2.4.3 Pressure Drop Constraint Equation

The solution to Equation 1 is constrained by a force balance which separates the total pressure drop along the flow path into five contributing mechanisms: pressure loss due to entrance effect, acceleration by vaporization, frictional effects, tortuosity of flow path and acceleration by changing flow area. All pressure drop equations were normalized by the pipe internal pressure in order to improve convergence.

$$\Omega(G_c^2, p_c) = (p_0 - p_c) - \Delta p_e - \Delta p_a - \Delta p_f - \Delta p_k - \Delta p_{aa} = 0 \quad (\text{Equation 3})$$

where

$p_0$  = absolute stagnation pressure of the subcooled liquid at the crack entrance of the pipe [Pa]

$p_c$  = absolute pressure at the crack exit [Pa]

$\Delta p_e$  = pressure loss due to entrance effects [Pa]

$\Delta p_a$  = pressure loss due to acceleration by vaporization [Pa]

$\Delta p_f$  = pressure loss due to frictional effects [Pa]

$\Delta p_k$  = pressure loss due to tortuosity of flow path [Pa]

$\Delta p_{aa}$  = pressure loss due to acceleration by changing flow area [Pa]

The following subsections present the equations that are used to calculate the individual contributions to the total pressure drop.

#### 2.4.3.1 Entrance Pressure Loss: $\Delta p_e$

$$\Delta p_e = \frac{G_c^2 v_{l(0)}}{2C_D^2} \left( \frac{A_c^2}{A_0^2} \right) \quad (\text{Equation 4})$$

where

$G_c$  = mass flux at the crack exit plane (aka choking or throat plane); [kg/m<sup>2</sup>-sec]

$v_{l(0)}$  = specific volume of subcooled liquid at crack entrance plane; [m<sup>3</sup>/kg]

$C_D$  = discharge coefficient  $0.60 \leq C_D \leq 0.95$  [-]

$A_0$  = flow area at crack entrance plane [m<sup>2</sup>]

$A_c$  = flow area at the throat [m<sup>2</sup>]

In the SQUIRT implementation,  $C_D$  is set to 0.95 [31] which is representative of smooth-edged or rounded entrances. In a similar extension of the Henry-Fauske model which also addresses pressure loss terms, called the *Abdollahian Model I* by John et al. [41],  $C_D$  is set to 0.62 which is representative of sharp-edged entrances. LEAPOR follows the SQUIRT implementation and sets  $C_D$  to 0.95. The potential effect on the calculated leakage rate and uncertainty introduced is discussed in Section 2.9

### 2.4.3.2 Phasic Acceleration Pressure Loss: $\Delta p_a$

$$\Delta p_a = G_c^2 \left( \frac{A_c}{A_i} \right) \left( \frac{A_c}{A_0} \right) \left[ (1 - x_{c(h)}) v_{f(c)} + x_{c(h)} v_{g(c)} - v_{f(0)} \right] \quad (\text{Equation 5})$$

where

- $A_c$  = flow area at the crack exit plane (at  $z = L$ ); [ $\text{m}^2$ ]
- $A_0$  = flow area at the crack entrance plane (at  $z = 0$ ); [ $\text{m}^2$ ]
- $A_i$  = flow area where vapor generation begins (at  $12D_h$ ); [ $\text{m}^2$ ]
- $v_{f(0)}$  = specific volume of subcooled liquid at crack entrance plane; [ $\text{m}^3/\text{kg}$ ]
- $v_{f(c)}$  = specific volume of saturated liquid at throat; [ $\text{m}^3/\text{kg}$ ]
- $v_{g(c)}$  = specific volume of saturated vapor at throat; [ $\text{m}^3/\text{kg}$ ]
- $x_{c(h)}$  = isenthalpic equilibrium vapor quality at the crack exit plane [-]

The assumed linear variation of the cross-sectional flow area along the flow path is

$$A(z) = A_0 + \left( \frac{z}{L} \right) (A_c - A_0) \quad (\text{Equation 6})$$

where

- $z$  = distance along flow path from the crack entrance [m]
- $L$  = total length of the flow path [m]
- $A_0$  = flow area at crack entrance plane (at  $z = 0$ ) [ $\text{m}^2$ ]

Therefore,  $A_i$  is for  $z = 12D_h$

$$A_i = A_0 + \left( \frac{12D_h}{L} \right) (A_c - A_0) \quad [\text{m}^2] \quad (\text{Equation 7})$$

where the hydraulic diameter,  $D_h$ , of the crack entrance flow area is defined by

$$D_h = \frac{4A_0}{P_w} \quad [\text{m}] \quad (\text{Equation 8})$$

$P_w$  = wetted perimeter of the flow area [m]

### 2.4.3.3 Frictional Pressure Loss: $\Delta p_f$

For the condition when  $L/D_h \geq 12$ , where  $D_h$  is the hydraulic diameter evaluated at the exit plane, the frictional pressure drop is calculated by

$$\Delta p_f = \frac{G_c^2}{2} \left\{ 12f \left( \frac{A_c^2}{A_i A_o} \right) v_{l(0)} + f \left( \frac{L}{D_h} - 12 \right) \left( \frac{A_c}{A_i} \right) [\bar{v}_f + \bar{x}_{(h)} \bar{v}_{fg}] \right\} \quad (\text{Equation 9})$$

where

- $G_c^2$  = mass flux at the crack exit plane
- $f$  = Darcy friction factor (see Equation 11)
- $A_c$  = flow area at the crack exit plane
- $A_i$  = flow area where vapor generation begins
- $A_o$  = flow area at the crack entrance plane
- $v_{l(0)}$  = specific volume of subcooled liquid at the crack entrance plane
- $L$  = total flow path length
- $D_h$  = hydraulic diameter (see Equation 8)
- $\bar{v}_f$  = saturated liquid specific volume at average pressure
- $\bar{x}_{(h)}$  = isenthalpic vapor quality at average pressure
- $\bar{v}_{fg}$  = change in specific volume by vaporization at average pressure

When  $L / D_h < 12$ , then the frictional pressure drop is calculated by

$$\Delta p_f = \frac{G_c^2}{2} \left\{ 12f \left( \frac{A_c^2}{A_i A_o} \right) v_{l(0)} \right\} \quad (\text{Equation 10})$$

The Darcy friction factor,  $f$  (see also Figure 2) is calculated by

$$f = \left[ C_1 \log_{10} \left( \frac{D_h}{\mu} \right) + C_2 \right]^{-2} \quad (\text{Equation 11})$$

The hydraulic diameter to effective surface roughness is limited by

$$\frac{D_h}{\mu} = \text{MAX} \left( \frac{D_h}{\mu}, 3.65 \right) \quad (\text{Equation 12})$$

where  $\mu$  is the effective surface roughness defined by Equation 15 and the hydraulic diameter ratio by Equation 19. The C coefficients are defined as:

$$\left. \begin{array}{l} C_1 = 2 \\ C_2 = 1.14 \end{array} \right\} \text{ for } \frac{D_h}{\mu} > 100 ; \quad \left. \begin{array}{l} C_1 = 3.39 \\ C_2 = -0.866 \end{array} \right\} \text{ for } \frac{D_h}{\mu} \leq 100;$$

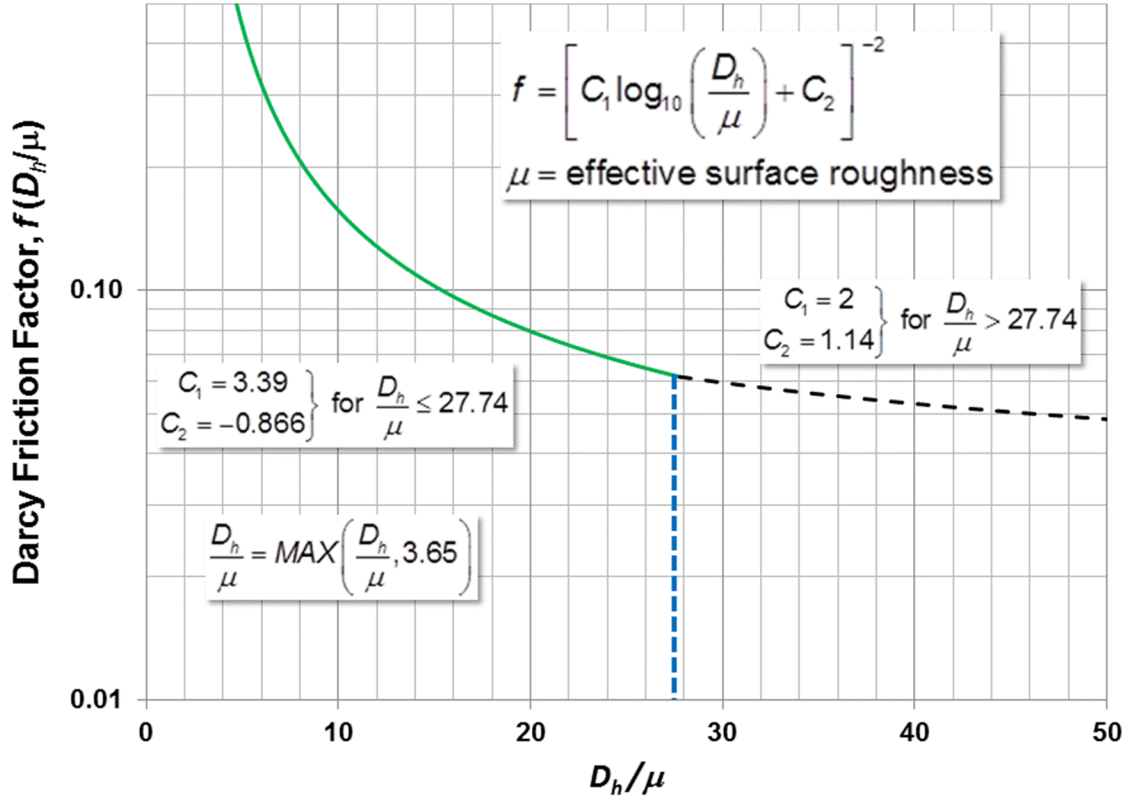


Figure 2. Implementation of Darcy friction factor,  $f$ , as a function of the ratio of the hydraulic diameter,  $D_h$ , to the effective surface roughness,  $\mu$ .

#### 2.4.3.4 Flow Path Tortuosity Pressure Loss: $\Delta p_k$

The tortuosity loss is influenced by the crack-face surface morphology.

$$\Delta p_k = e_{\text{vloss}} \frac{G_c^2}{2} \left( \frac{A_c}{A_f} \right) \left[ (1 - \bar{x}_{(h)}) \bar{v}_f + \bar{x}_{(h)} \bar{v}_g \right] \quad (\text{Equation 13})$$

Where the expression for  $e_{\text{vloss}}$  is defined as

$$e_{\text{vloss}} = \eta_t \left( \frac{L_{\text{eff}}}{L} \right) L = \eta_t L_{\text{eff}} \quad (\text{Equation 14})$$

In addition to the crack-opening displacement,  $\delta_{\text{COD}}$ , the loss term,  $e_{\text{vloss}}$ , is a function of several crack-face surface morphology parameters described in Section 0.



#### 2.4.3.4.1 Crack Morphology Parameters

The crack morphology parameters were developed to further account for the pressure loss due to flow path tortuosity by developing parameters that are a function of the crack opening diameter. These parameters are:

- $\mu$ ,  $\mu_L$ ,  $\mu_G$  = effective, local and global surface roughness, respectively
- $\eta_t$ ,  $\eta_{tL}$  = effective and local number of turns in the flow path, respectively
- $K_G$ ,  $K_{G+L}$  = global and local factor for flow path deviation from straight, respectively

The effective surface roughness,  $\mu$ , required for the Darcy friction factor,  $f$ , is a function of crack-opening displacement,  $\delta_{COD}$ ,

$$\mu = \begin{cases} \mu_L & \text{for } 0 < \frac{\delta_{COD}}{\mu_G} \leq 0.1 \\ \mu_L + \frac{(\mu_G - \mu_L)}{9.9} \left[ \frac{\delta_{COD}}{\mu_G} - 0.1 \right] & \text{for } 0.1 \leq \frac{\delta_{COD}}{\mu_G} < 10 \\ \mu_G & \text{for } \frac{\delta_{COD}}{\mu_G} \geq 10 \end{cases} \quad (\text{Equation 15})$$

The effective number of turns per unit length,  $\eta_t$ , is also a function of crack-opening displacement,  $\delta_{COD}$ ,

$$\eta_t = \begin{cases} \eta_{tL} & \text{for } 0 < \frac{\delta_{COD}}{\mu_G} \leq 0.1 \\ \eta_{tL} - \frac{(\eta_{tL})}{11} \left[ \frac{\delta_{COD}}{\mu_G} - 0.1 \right] & \text{for } 0.1 \leq \frac{\delta_{COD}}{\mu_G} < 10 \\ 0.1 \eta_{tL} & \text{for } \frac{\delta_{COD}}{\mu_G} \geq 10 \end{cases} \quad (\text{Equation 16})$$

and the ratio of adjusted flow path length,  $L_{eff}$ , to pipe wall thickness,  $L$ , is

$$\frac{L_{eff}}{L} = \begin{cases} K_{G+L} & \text{for } 0 < \frac{\delta_{COD}}{\mu_G} \leq 0.1 \\ K_{G+L} - \frac{(K_{G+L} - K_G)}{9.9} \left[ \frac{\delta_{COD}}{\mu_G} - 0.1 \right] & \text{for } 0.1 \leq \frac{\delta_{COD}}{\mu_G} < 10 \\ K_G & \text{for } \frac{\delta_{COD}}{\mu_G} \geq 10 \end{cases} \quad (\text{Equation 17})$$

A series of computational fluid dynamic (CFD) numerical experiments are presented in Appendix C of NUREG/CR-6861 [23] and provide the technical basis for the implementation of the crack morphology parameters as a function of the crack-opening displacement (COD) and global surface roughness.

#### 2.4.3.5 Pressure Loss Due to Acceleration from Changing Flow Area: $\Delta p_{aa}$

$$\Delta p_{aa} = \frac{G_c^2 V_{l(0)}}{2} \left[ \left( \frac{A_c}{A_i} \right)^2 - \left( \frac{A_c}{A_0} \right)^2 \right] + \frac{G_c^2}{2} \left[ (1 - \bar{x}_{(h)}) \bar{v}_f + \bar{x}_{(h)} \bar{v}_g \right] \left[ 1 - \left( \frac{A_c}{A_i} \right)^2 \right] \quad (\text{Equation 18})$$

where

$A_0$  = flow area at crack entrance plane (at  $z = 0$ )

$A_c$  = flow area at the crack exit plane (at  $z = L$ )

$A_i$  = flow area at  $z = 12D_h$ ;

$$A_i = A_0 + \left( \frac{12D_h}{L} \right) (A_c - A_0)$$

$\bar{v}_f$  = specific volume of saturated liquid at average pressure,  $p_{avg}$ ; [ $\text{m}^3/\text{kg}$ ]

$\bar{v}_g$  = specific volume of saturated vapor by vaporization at the average pressure,  $p_{avg}$ ; [ $\text{m}^3/\text{kg}$ ]

$$p_{avg} = \frac{p_0 - \Delta p_e + p_c}{2}; [\text{Pa}]$$

#### 2.4.4 Shapes of Cross-Sectional Flow Area of Crack Channel

LEAPOR offers three different cross-sectional flow area shapes: a rectangle, a diamond or an ellipse. Figure 3 shows these cross-sectional shapes, each with an aspect ratio ( $a/b$ ) of approximately 4. For Use Case 2, which is the Use Case the xLPR Code utilizes only the elliptical cross-sectional shape option is available. In addition to the cross-sectional mean flow area,  $A_{xmf}$ , the hydraulic diameter,  $D_h$ , of the crack channel must be calculated for each shape, where

$$D_h = \frac{4A_{xmf}}{P_w} \quad (\text{Equation 19})$$

and  $P_w$  is the wetted perimeter. As depicted in Figure 3, the calculation of these parameters for the rectangle and diamond is straightforward; however, the calculation of the wetted perimeter for an ellipse is much more complex. For the ellipse,

$$P_w = 4aE(e)$$

$E(e)$  = complete elliptic integral of the second kind

$$e = \frac{\sqrt{a^2 - b^2}}{a} = \text{eccentricity of the ellipse}$$

(Equation 20)

where  $a$  is the *semi-major* axis and  $b$  is the *semi-minor* axis of the ellipse. The Gauss-Kummer series of  $h$  infinite series representation was implemented in the LEAPOR coding using Horner's rule to approximate the circumference of an ellipse.

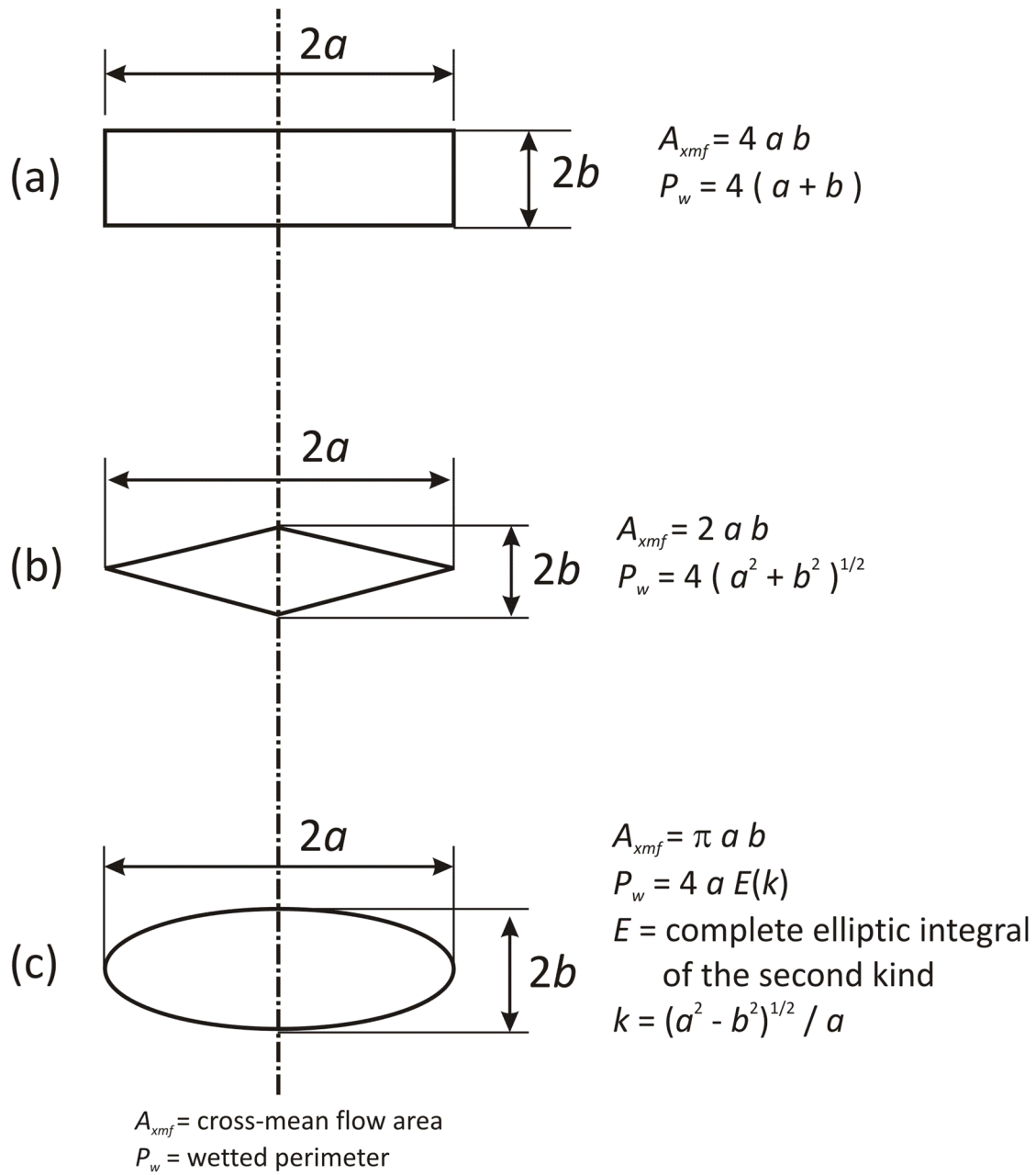


**Figure 3. Crack flow area shapes: (a) rectangle, (b) diamond and (c) ellipse**

## 2.4.5 Transition Model

The Henry-Fauske thermohydraulic model is valid only for tight cracks [16-18]. Several SQUIRT References [37-40] identify the region of applicability for the Henry-Fauske two-phase thermal-hydraulic model as depicted in Figure 4 (taken from ref. 38). Crack geometries with  $L/D_h > 15$  represent tight cracks where the Henry-Fauske model may be applied to estimate choked two-phase flow rates. For wider cracks with  $L/D_h < 0.5$ , an orifice flow model using single phase liquid properties can be applied. The region defined by  $0.5 \leq L/D_h \leq 15$  requires the construction of a *transition model* to link tight-crack two-phase flows with wide-crack single-phase (liquid) flows. [SR-LRM-010, SR-LRM-011]

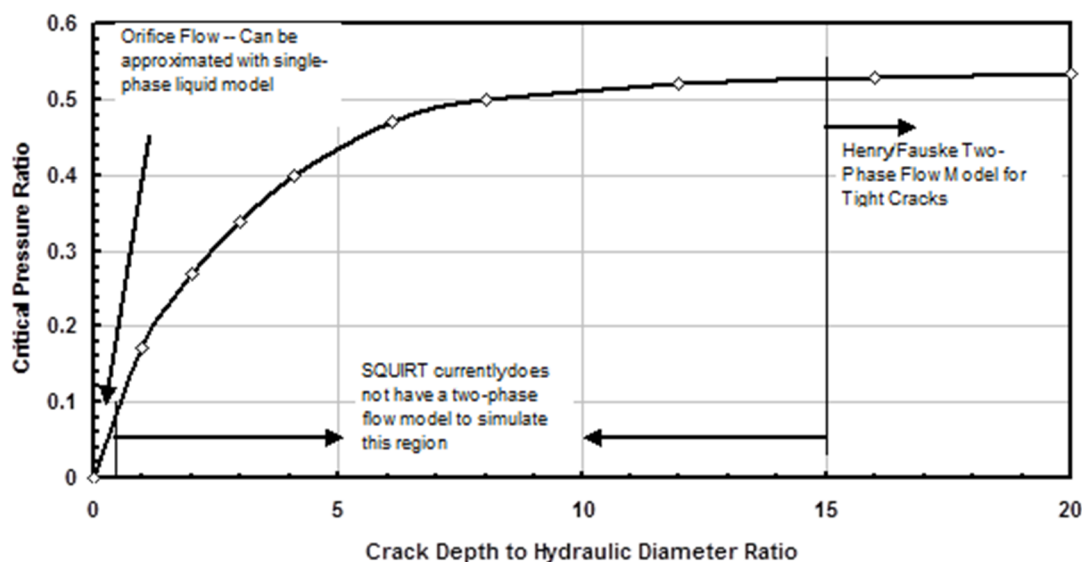


**Figure 4.** (Fig. 4 from ref. 38 ) Plot of critical pressure ratio as a function of the ratio of the crack depth (i.e., pipe wall thickness,  $L$ ) to hydraulic diameter,  $D_h$ , showing when the leak rate models in SQUIRT are valid and when they are not.

Such a transition model was developed for the MERIT Program and is presented in ref. 37. In this transition model, the regions of applicability have been modified from earlier versions of SQUIRT to cover the full range of crack sizes from very tight cracks ( $L/D_h > 30$ ) to wide cracks ( $L/D_h < 4.6$ ). For the implementation of this transition model into LEAPOR, the pipe wall thickness,  $L$ , used in ref. 37 was replaced by the effective flow path length,  $L_{eff}$ , as defined by Equation 17 to be consistent with the surface morphology model and its dependence on crack-opening-displacement. The transition model as presented in Reference 37 and implemented in LEAPOR is shown in Figure 5 and Figure 6 divided into the four flow regimes defined in Section 2.4.5.1.

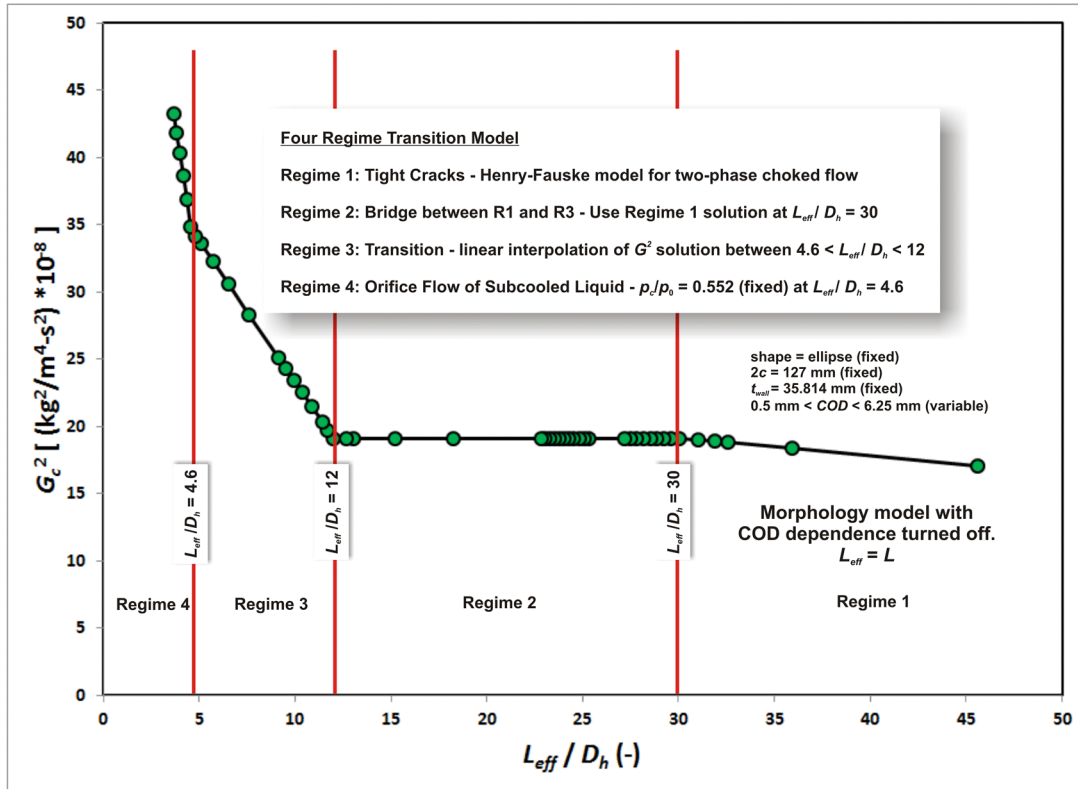


Figure 5. Transition Model – regime definitions (morphology model turned off).

#### 2.4.5.1 Transition Model – Definition of Four Flow Regimes

Figure 5 shows the four-regime transition model where the boundaries of each regime are defined by the geometric parameter  $L_{eff}/D_h$ .

- Regime 1 – ( $L_{eff}/D_h \geq 30$ ); tight cracks with two-phase choked flow as simulated by the Henry-Fauske model.
- Regime 2 –  $12 \leq L_{eff}/D_h < 30$ ; a bridge between Regimes 1 and 3, where the mass flux,  $G_c$ , calculated at  $L_{eff}/D_h = 30$  in Regime 1 is assumed constant. Changes required to project back to  $L_{eff}/D_h = 30$  and calculate the assumed constant mass flux for this regime are accomplished by adjustments to the inner and outer  $\delta_{COD}$  only. The pipe wall thickness,  $L$ , and crack length,  $2c$ , remain fixed.
- Regime 3 –  $4.6 < L_{eff}/D_h < 12$ ; a transition region between two-phase choked flow and single-phase liquid orifice flow using a linear interpolation of the square of the mass flux,  $G_c^2$ , with  $L_{eff}/D_h$  as the interpolant variable. The value at  $L_{eff}/D_h = 4.6$  is determined by Regime 4.

- Regime 4 –  $L_{eff} / D_h \leq 4.6$ ; wide cracks with orifice flow of single-phase liquid, where the critical pressure<sup>3</sup> ratio of  $p_c / p_o$  is assumed to be a linear function of  $L_{eff} / D_h$ . To complete the model definition, the value of  $p_c / p_o$  at  $L_{eff} / D_h = 4.6$  is assumed fixed at 0.552, and  $p_c / p_o = 0$  at  $L_{eff} / D_h = 0$ . Subcooled liquid water properties are determined at the pressure and temperature inside the pipe ( $p_o, T_o$ ).

#### 2.4.5.2 Influence of COD-Dependent Morphology Model

In the implementation of the Transition Model, the effective length,  $L_{eff}$ , of the crack flow path replaces the pipe wall thickness,  $L$  in order to maintain consistency with the surface morphology model. Through the ratio that the surface morphology parameters are a function of,  $\delta_{COD}/\mu$ , a second transition model demonstrates an influence on the flow rates predicted in Regime 1. This effect can be observed in Regime 1 in Figure 6 where for  $\delta_{COD}/\mu \leq 10$  there is a rapid rate of change in the predicted flow rate with increasing  $L_{eff}/D_h$  (caused by a decreasing  $\delta_{COD}$ ). In the region with  $\delta_{COD}/\mu > 10$ , the flow rate continues to rise as it approaches  $L_{eff}/D_h = 30$ , but at a much reduced rate.

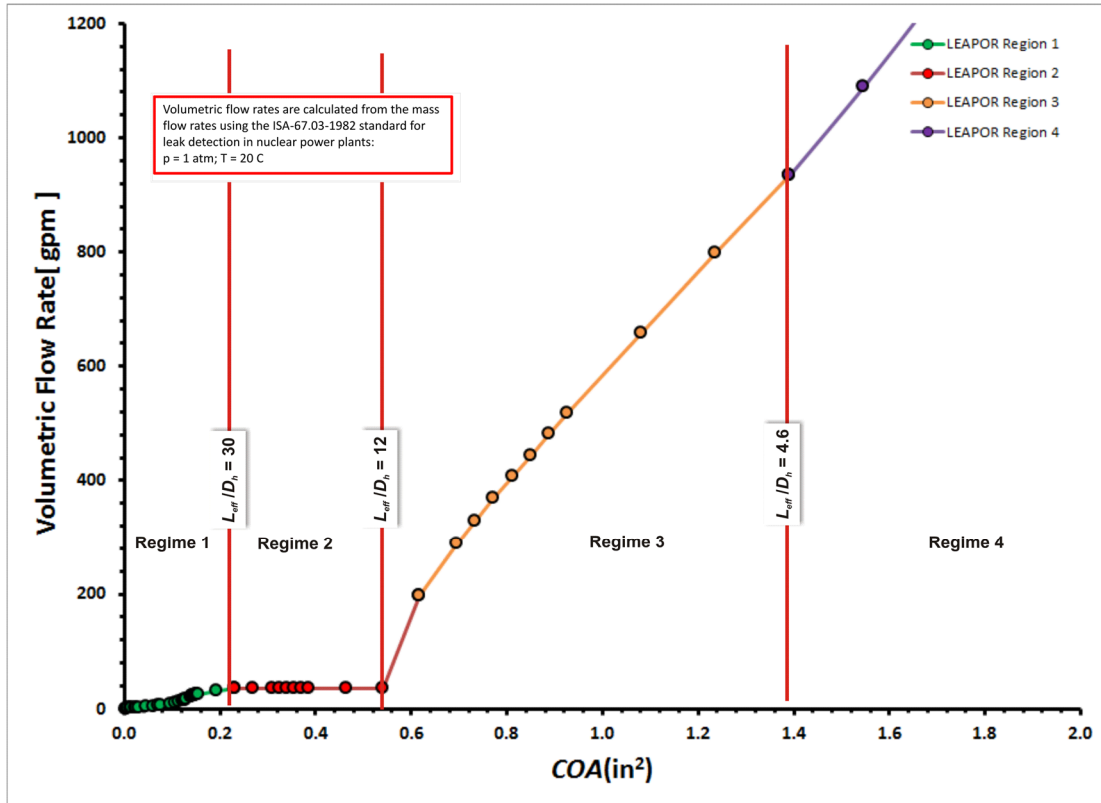


Figure 6. Transition Model – regimes mapped onto volumetric flow rate (morphology model turned on)

<sup>3</sup> Since the fluid in Regime 4 is in a subcooled or metastable liquid phase, a choked flow state cannot be attained. The liquid phase is assumed incompressible, and the acoustic celerity is, therefore, infinite. The use of the variable,  $p_c$ , previously associated with the concept of critical pressure for a choked flow state is not quite correct here, but it will serve for the purposes of defining the model.

## 2.4.6 Orifice Flow Model

Regime 4 treats the wide crack as a thin square-edged orifice [6] where the subcooled liquid is assumed to be incompressible. The equation implemented into LEAPOR for estimated orifice flow rates is

$$Q = \frac{C_D A_0 \sqrt{2 \Delta p v_{l(0)}}}{\sqrt{1 - \beta^4}} \quad (\text{Equation 21})$$

using  $C_D=0.6$  and  $\beta=0.62$ . As described in the definition for Regime 4 in Section 2.4.5.1 the critical pressure ratio  $p_c/p_o$  is fixed at 0.552 at  $L_{eff}/D_h=4.6$ . If a linear dependence on  $L_{eff}/D_h$  is assumed then the required pressure loss is

$$p_0 - p_c = \Delta p = p_0 \left[ 1 - \left( \frac{0.552}{4.6} \right) \left( \frac{L_{eff}}{D_h} \right) \right]; \text{ for } \frac{L_{eff}}{D_h} \leq 4.6 \quad (\text{Equation 22})$$

Applying Equation 22 to Equation 21, one can then solve for the mass flux at the entrance to the crack, such that

$$G_0 = \frac{Q}{v_{l(0)} A_0} = \frac{C_D \sqrt{2 \Delta p v_{l(0)}}}{v_{l(0)} \sqrt{1 - \beta^4}}; \left[ \frac{\text{kg}}{\text{m}^2 - \text{sec}} \right] \quad (\text{Equation 23})$$

where  $v_{l(0)}$  is, as defined before, the specific volume of the subcooled liquid at the crack entrance.

## 2.5 Solution Strategy

The two solution variables to be calculated by the model are the mass flux,  $G_c$ , and pressure,  $p_c$ , both at the exit plane of the crack. All other variables are either input data, functions of the two solution variables, or functions of empirical relations. Equations 1 and 3 with supporting equations represent a closed, coupled set of two non-linear equations with two unknowns. The classic iterative procedure for solving non-linear systems is called Newton's method. The primary advantage of Newton's method is that, given a suitable initial guess the resulting sequence of solution vectors exhibits a locally quadratic convergence to the true solution. The primary disadvantage with Newton's method is that a general initial guess of the solution vector does not ensure a globally convergent process; i.e., a suitable initial guess is not known *a priori*. If the initial guess is too far away from the true solution in the solution space, the solution vector sequence may possibly diverge or converge to the wrong solution. Modified Quasi-Newton methods are available that attempt to adjust the procedure to exhibit a more globally convergent character and to help guide the iterations to the correct solution. The Quasi-Newton-based solution procedure selected for this baseline implementation of the leak rate module is called the *trust region method*. The mathematical details and description of the Trust Region Method can be found in the Leak Rate Module SDD [48].

## 2.6 Thermodynamic Properties of Water

The leak rate model requires the accurate and computationally-efficient determination of certain thermodynamic properties of water as a subcooled liquid, saturated liquid, wet and saturated steam, and dry (superheated) steam. Such "steam tables" have been implemented in Fortran

source code by a number of organizations. The ASME IAPWS-IF97 Steam Properties for Industrial Use<sup>4</sup> (released in 1997) provides an implementation of the International Association of Properties of Water and Steam (IAPWS) formulation. This Fortran library was purchased from ASME and resides in the Properties Layer of LEAPOR. The ASME has granted permission to use this Fortran library in LEAPOR.

## 2.7 Numerical Approximation of Derivatives

It is required in the implementation of the leak rate model that derivatives be calculated. This operation may be carried out analytically where possible or numerically through the application of finite difference ratios. The following first, second, and fourth-order finite-difference approximations [12] were implemented in the code and tested for suitability:

$$\text{Forward Difference: } \left. \frac{df}{dx} \right|_{x_1} \approx \frac{f(x_1 + \delta x) - f(x_1)}{\delta x}; O(\delta x)$$

$$\text{Backward Difference: } \left. \frac{df}{dx} \right|_{x_1} \approx \frac{f(x_1) - f(x_1 - \delta x)}{\delta x}; O(\delta x)$$

$$\text{Central Difference: } \left. \frac{df}{dx} \right|_{x_1} \approx \frac{f(x_1 + \delta x) - f(x_1 - \delta x)}{2\delta x}; O(\delta x^2)$$

$$\text{Central Difference: } \left. \frac{df}{dx} \right|_{x_1} \approx \frac{f(x_1 - 2\delta x) - 8f(x_1 - \delta x) + 8f(x_1 + \delta x) - f(x_1 + 2\delta x)}{12\delta x}; O(\delta x^4)$$

## 2.8 Different Inner and Outer Diameter Crack-Opening Areas

For the preprocessing mode (Use Case 2) it is required that a correction be applied to the leakage rate value determined from the table when the crack-opening areas (COA) on the inner and outer diameter surface differ [SR-LRM-014]. Based on analyses, the correction will be applied only in cases in which the thickness to hydraulic diameter ratio is greater than 30, i.e. the flow is in Regime 1. Therefore, when the leak rate module is called, the Framework will determine the leakage rate from the leak rate tables using the inner diameter crack length and COD, interpolating if necessary. Then the Framework will check if the thickness to hydraulic diameter ratio is greater than 30. If this is true, the Framework will determine the leakage rate from the leak rate tables using the outer diameter crack length and COD and then average this value with the inner diameter leakage rate. A flow chart visualizing this process is shown in Section 3.5 and the correction method is defined in Section 2.8.1.

### 2.8.1 Correction Method

The correction to be applied to the leak rate value found in the leakage rate tables is a function of the regime in which the flow is determined to exist. The flow regime is determined by the ratio of the pipe thickness (the approximate flow path length) and the hydraulic diameter. The correction is applied only when the flow is determined to be in Regime 1. When the flow is in Regimes 2, 3, or 4, the deviation from the idealized leak rate value found in the leakage rate tables using the inner diameter crack length and COD (when COA\_inner = COA\_outer) is

---

<sup>4</sup> [http://committees.asme.org/K&C/TCOB/BRTD/WSTS/Properties\\_Steam\\_Subcommittee.cfm](http://committees.asme.org/K&C/TCOB/BRTD/WSTS/Properties_Steam_Subcommittee.cfm)



insignificant and can be ignored. Figure 7 shows the deviation from the actual crack leak rate (the leak rate calculated using the actual crack length and COD values on the inner diameter and the actual crack length and COD values on the outer diameter) when the idealized inner diameter crack length and COD are used (blue data series) and when the idealized outer diameter crack length and COD are used (red data series). For large leak rates, which correspond to those outside of Regime 1, if the inner diameter crack length and COD are used without any correction, the leak rate predicted by the idealized crack will be very close to the actual leak rate as shown in Figure 7(a). Therefore for Regimes 2, 3, and 4 the inner diameter crack length and COD will be used to look up the leak rate from the leak rate tables and no correction will be applied.

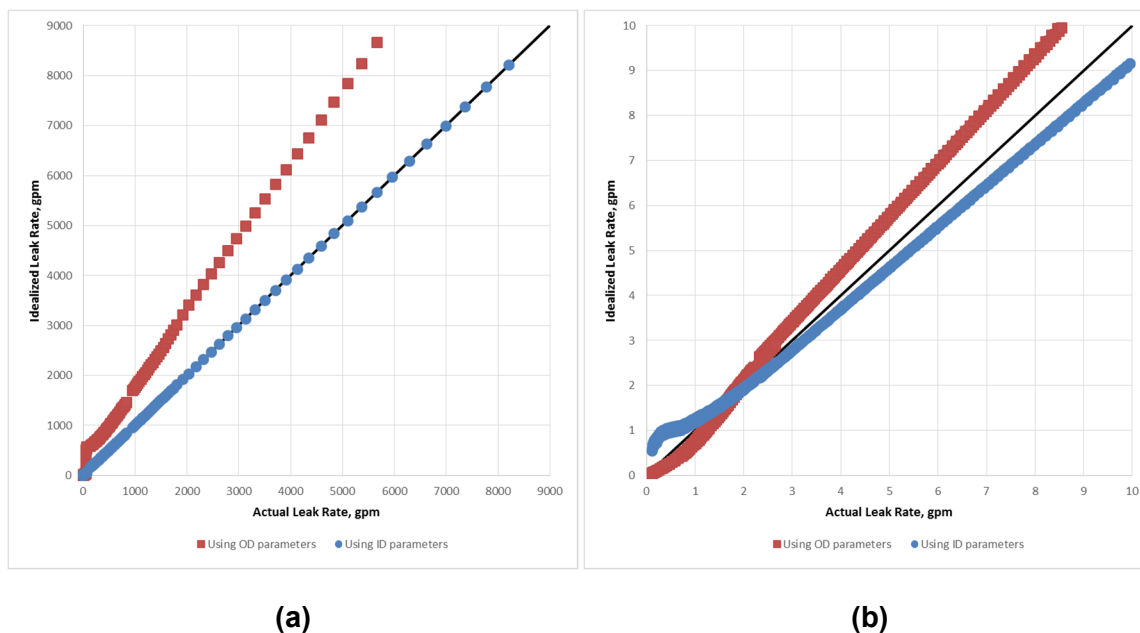


**Figure 7. Deviation of the idealized leak rate using the inner diameter values (blue) or outer diameter values (red) over all calculated leak rates (a) and focusing on low leak rates (b).**

For low leak rates using the inner diameter crack length and COD does not provide a good estimate of the actual leak rate as shown in Figure 7(b). However, it does appear that if the average of the idealized inner diameter leak rate and the idealized outer diameter leak rate is used then the result will be close to the actual leak rate. Therefore, this correction is applied and the resulting leak rate is compared to the actual leak rate in Figure 8 over all calculated leak rates (a) and focusing on low leak rates (b).

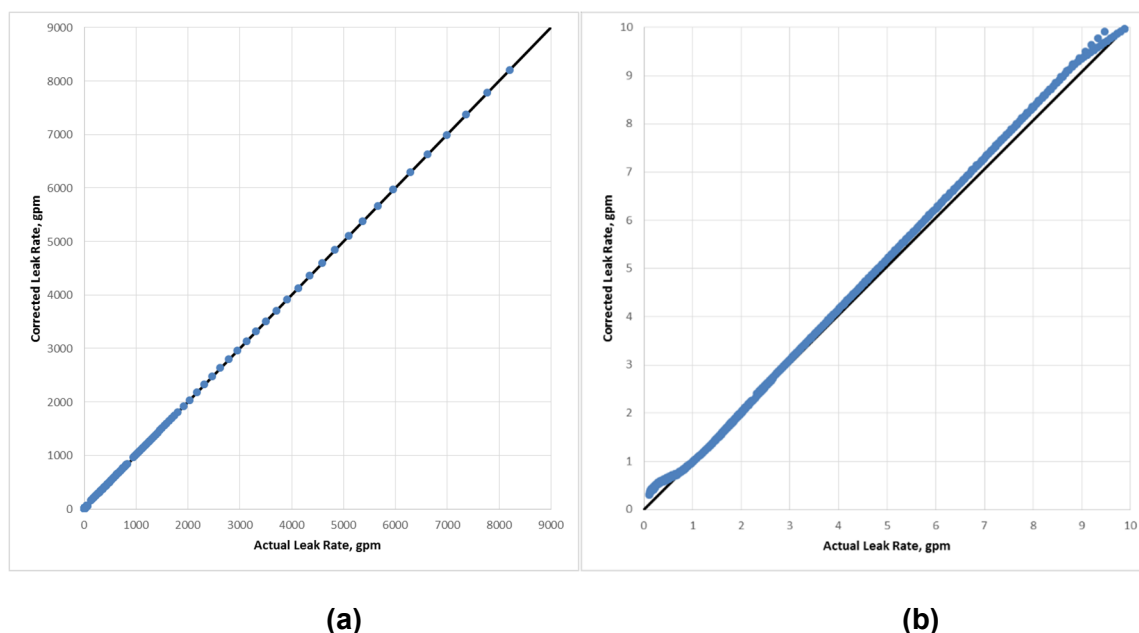


**Figure 8. Deviation of the corrected leak rate from the actual leak rate over all calculated leak rates (a) and focusing on low leak rates (b) .**

As Figure 8 shows, using the average of the idealized crack inner diameter leak rate and the idealized crack outer diameter leak rate when the flow is in Regime 1 and using the idealized crack inner diameter leak rate for all other regimes, predicts the actual leak rate with very good accuracy.

## 2.9 Uncertainty

### 2.9.1 Discharge Coefficient

It is known that there is significant uncertainty in the crack morphology variables but the uncertainty in the leakage due to the discharge coefficient,  $C_D$ , has not been investigated. The discharge coefficient is the ratio of the flow area of the vena contracta near the entrance to the flow area at the crack channel entrance plane. This coefficient is used in determining the pressure loss due to entrance effects per Equation 4 in Section 2.4.3.1. LEAPOR uses a value of 0.95 which is representative of rounded entrances. The technical basis for using a value of 0.95 is based on the assumption that, at the small length scales typically associated with a tight crack, the edges of the entrance plane will appear rounded or smooth relative to the small length scales of the inner surface morphology of the crack channel near the entrance. LEAPOR was run with the inputs shown in Table 5 along with 825 different inner and outer crack length and crack-opening diameter combinations that ran through all four regimes defined in LEAPOR for discharge coefficients of 0.95, 0.8, 0.7 and 0.6.

**Table 5. Input parameters for  $C_D$  test cases**

Outer radius (mm)	431
thickness (mm)	60.2
Pressure (MPa)	15.4
Temperature (°C)	340
Global roughness ( $\mu\text{m}$ )	113.9
Local roughness ( $\mu\text{m}$ )	16.86
Number of turns (1/m)	5940
Global path deviation factor	1.009
Local path deviation factor	1.243

The percent error is defined as the deviation from the leakage rate calculated when the implemented value of 0.95 for the discharge coefficient is used. The maximum percent error for each varying discharge coefficient is shown in Table 6.

**Table 6. Maximum percent error for varying  $C_D$** 

$C_D$ value	Maximum % error
0.8	0.46
0.7	0.93
0.6	1.63

Since the maximum percent error is 1.63% for all cases, any uncertainty in the value of the discharge coefficient can be ignored.

## 2.9.2 Crack Morphology Variables

In order to characterize the uncertainty in the leakage rate due to the crack morphology variables PROMETHEUS[32] was run for the combinations of (1) maximum pressure and maximum temperature, (2) maximum pressure and minimum temperature, (3) minimum pressure and maximum temperature, and (4) minimum pressure and minimum temperature while keeping all input variables other than the crack morphology variables constant. The coefficient of variation (COV), defined as the ratio of the standard deviation of the leak rate to the mean leak rate, will be used to quantify the uncertainty by characterizing only the effect from variations in the crack morphology parameters. If there is no crack morphology (i.e., polished surfaces) then the COV is zero. The PROMETHEUS code is used because the code has integrated LEAPOR into the probabilistic model for leak detection and thus the impact of different crack depths, crack lengths, COD and COA on leak rate can all be investigated. For PWSCC, the crack growth is significantly impacted by temperature so one cannot assume crack lengths and depths independently of the temperature. The COV is then plotted as a function of the mean leak rate. These plots are shown in Figure 9.

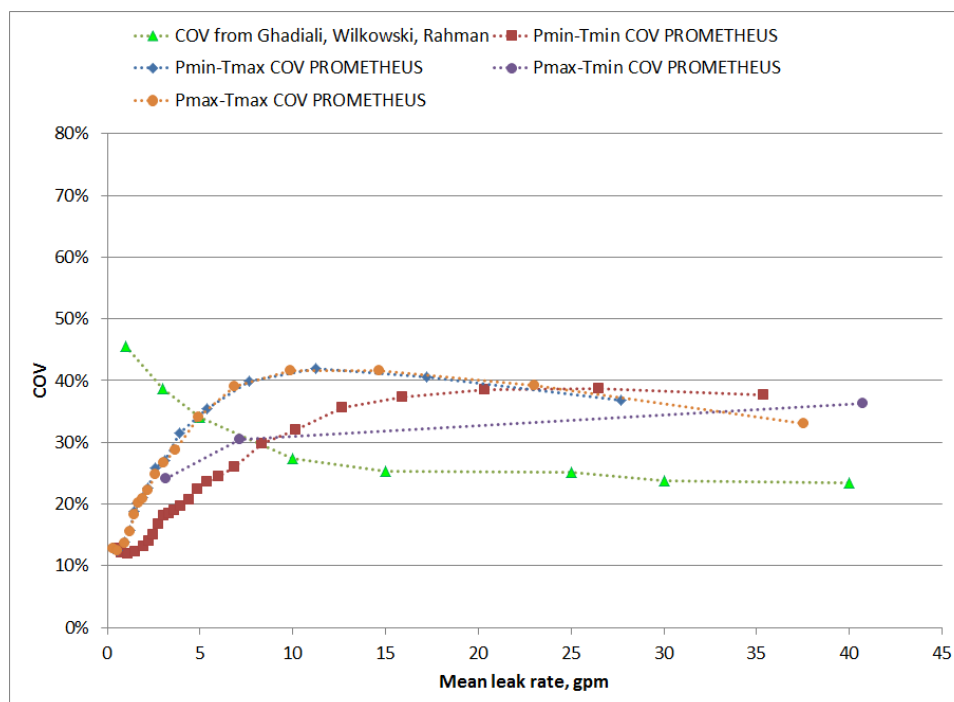


**Figure 9. Power law fit to the COV as a function of the mean leak rate for the four pressure temperature combinations**

As this figure shows, the trend observed in the PROMETHEUS study is exactly the opposite of what was found previously by Ghadiali et al [14]. That is, when the mean leak rate is low the COV is relatively high, but in this analysis the COV is relatively low when the mean leak rate is low. To address this situation we examined a Bayesian updating of the work by Ghadiali, et al. [14] When we combine the current analyses with theirs we get the results in Figure 10.

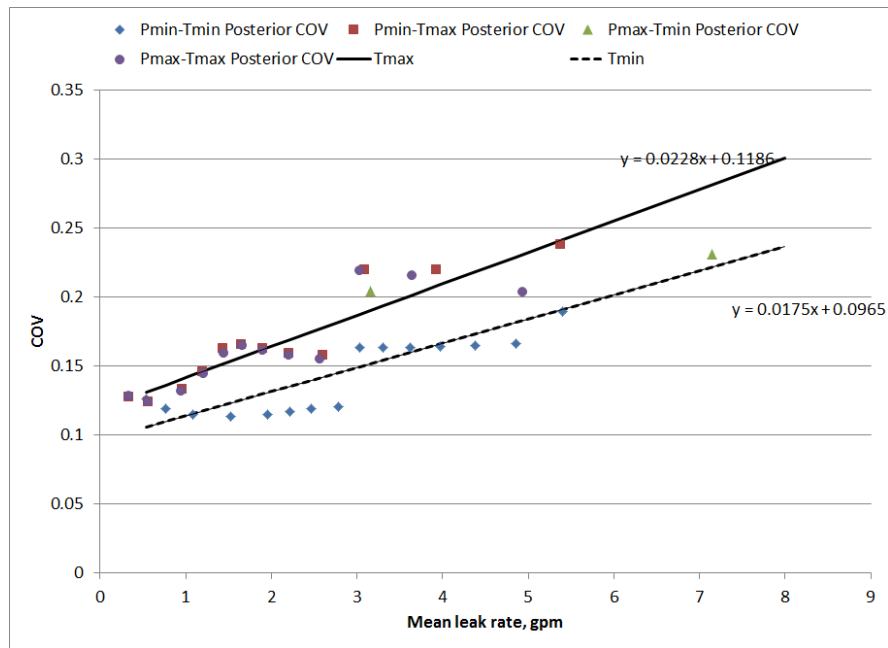


**Figure 10 Relationship for the COV as a function the mean leak rate and the temperature**

Examination of Figure 9 indicates that once the mean leak rate is greater than 8 – 10 gpm the COV “flat lines” at about 25%. Below this value there is a difference between the minimum temperature and maximum temperature results. This is shown in Figure 10.

Therefore, based on the results shown in Figure 10, for a mean leak rate  $\lambda$ , the standard deviation in linear space is to be interpolated between the 280°C (Equation 24) and 340°C equations (Equation 25):

$$\text{COV} = 0.0175\lambda + 0.0965 \quad (\text{Equation 24})$$

$$\text{COV} = 0.0228\lambda + 0.1186 \quad (\text{Equation 25})$$

Since the crack morphology parameters are only applied when the crack opening displacement to roughness ratio is small, i.e. for lower leakage rates, it is known that the COV will be zero for cases in which the crack morphology parameters are not applied, i.e. high leakage rates. Since we see the COV ‘flat line’ at around 8-10 gpm it is assumed that beyond 10 gpm there is no effect from morphology parameters and therefore the uncertainty (as measured by standard deviation) is 0. Since we do not want the uncertainty to drop suddenly at the 10 gpm limit, Equation 24 and Equation 25 are used to determine the COV value only when the leak rate is less than or equal to 4 gpm. Between 4 gpm and 10 gpm a linear fit between the COV value at 4 gpm and the COV value at 10 gpm is used to determine the COV value at the desired leak rate. The COV is then used by the Framework to sample the leakage rate to obtain its final value. More details on the leak rate uncertainty can be found in the Leak Rate Module SDD [53] and the Framework SDD [47].

## **3. LEAKAGE RATE MODEL IMPLEMENTATION**

### **3.1 Implementation Structure**

All preprocessing operations come under the responsibility of the xLPR Preprocessing application developed by the Computational Group. This Preprocessing application will read the user inputs for pipe diameter, pipe thickness, minimum and maximum pressure and minimum and maximum temperature from the Input Spreadsheet and call LEAPOR in single-case mode to calculate the required leak rates. The Leak Rate DLL wrapper coding was also developed by the Computational Group and is required to interface with both the GoldSim Framework application and the Preprocessor application. SQA documentation for the wrapper coding and preprocessor application is included in the Framework SQA documentation series.

For the preprocessing mode, the LEAPOR DLL will return two sets of tables of flow rates (in gpm and kg/sec) as a function of crack length ( $2c$  [mm]) and COD [mm]. Both tables will correspond to degradation types specified as user input. The dimensions of both tables are ( $Ninc_{2c} \times Ninc_{cod}$ ), where the variables  $Ninc_{2c}$  and  $Ninc_{cod}$  (automatically determined variables as required by [SR-LRM-016]) are the discretization for the crack length and COD, respectively. Each set of tables consists of four leakage rate tables in which the minimum and maximum values of pressure and temperature (given as user inputs or as default values provided as stated in [SR-LRM-015]) are used as bounds. Therefore, for each degradation type, there will be a set of leakage rate tables in which the following combinations will be used as inputs: minimum pressure and minimum temperature, minimum pressure and maximum temperature, maximum pressure and minimum temperature, and maximum pressure and maximum temperature. The tables assume that the crack length and COD on the inner and outer diameter are identical. For analyses in which the flow is in Regime 1 as defined in Section 2.4.5.1 a correction must be applied to the leakage rate value in the table as described in Section 2.8.1. Additionally, the leakage rate tables assume there is no uncertainty in the inputs when calculating the leak rates. In order to account for the uncertainty due to the crack morphology variables a factor is applied to the leakage rate value in the table as described in Section 2.9. These corrections are applied according to the flow diagram shown in Section 3.5.

### **3.2 Implementation of Model Requirements**

This section provides information on how each of the software requirements defined in Section 2.1 has been implemented into the Leak Rate Module.

#### **3.2.1 LEAPOR Code Development**

The development of the LEAPOR software code by Oak Ridge National Laboratory (ORNL) [27] addressed several of the Leak Rate Module requirements including:

- **SR-LRM-001** – Develop a software application that will calculate an estimate for the leakage rate of water escaping from a postulated through-wall crack in a piping segment of a nuclear power plant cooling water system.
- **SR LRM-002** – Implement the Henry-Fauske thermohydraulic model [13-15] that is used in the SQUIRT code [35] for tight cracks.
- **SR LRM-003** – The new application must be designed in such a way that the design attributes of maintainability, portability, and extensibility can be realized successfully by

future developers who were not necessarily involved in the original task of creating the software.

- **SR LRM-004** – The new application must comply with all xLPR Project Software Quality Assurance (SQA) requirements including evaluations for correctness, consistency, completeness, accuracy, readability, and testability, and be prepared to successfully meet the criteria of all SQA audits.
- **SR LRM-005** – Develop the Leakage Rate Module for two general use cases
  - Use Case 1: a standalone code with a human actor using a console application run from a blind prompt window, and
  - Use Case 2: an external DLL element where the actor is the GoldSim xLPR application or the preprocessor Excel Add-In application to be developed for the xLPR Excel Inputs Database. The same DLL shall be addressable by either actor. The Leakage Rate Module shall be embedded within DLL wrapper coding to be developed by the Computational Group.
- **SR LRM-006** – The required inputs and outputs are presented in Table 1 - Table 4
- **SR LRM-007** – Internally, the physical models will be implemented using the SI system of units. When required, all units conversions will be based on IEEE/ASTM SI 10™ 2010, American National Standard for Metric Practice [7].

The details of how the LEAPOR code addresses each of the above requirements can be found in the Leak Rate Module SDD [48].

### **3.2.2 SR-LRM-008 – For the standalone application (Use Case 1), develop a graphical user interface. This requirement can be delayed until time and resources become available for a future implementation.**

This requirement has been delayed and is not required for leakage rate calculations in the xLPR Code.

### **3.2.3 SR-LRM-009 – Develop a suite of internal unit tests that exercise all significant elements of the new application.**

A suite of internal test units has been developed that can be run every time the LEAPOR code is run in order to ensure the validity of particular elements of the software code. These unit tests include known solutions to test and ensure that the steam tables are returning correct values for the thermohydraulic properties, and the crack geometry class, error logging and the Nonmonotonic Nonlinear Equation Solver (NNES) [3] iteration scheme are working as intended. Although these unit tests can be run every time LEAPOR is executed since these unit tests are not problem-specific it is sufficient to run them once to determine that the application elements just described are functioning correctly.

### **3.2.4 Regime Definitions**

The Henry-Fauske model is valid only for the case of tight cracks and orifice flow models are valid only for the case of wide cracks. The flow regimes in between these cases require different

solutions. LEAPOR followed the structure of earlier leakage rate calculation software codes and divided the solution space into four flow regimes as defined in Section 2.4.5.1. These flow regimes are a function of the flow path length to the hydraulic diameter ratio. LEAPOR checks to determine if this ratio is less than 4.6, which corresponds to orifice flow conditions and if so calculates the leakage rate using Equation 23 defined in Section 2.4.6, thus addressing requirement SR-LRM-010. When the flow path length to hydraulic diameter ratio is greater than 30, the tight-crack Henry-Fauske thermohydraulic model can be used. In between these cases a linear interpolation scheme is implemented to model this transition as described in Section 2.4.5, and addressing requirement SR-LRM-011.

### **3.2.5 Error Codes**

Table 7 lists the LEAPOR Error Codes. Error codes 121-199 address requirement SR-LRM-012 by ensuring valid inputs. Error codes 215 and above address requirement SR-LRM-013 by returning messages for cases which are not physically valid or a solution cannot be found.



**Table 7. LEAPOR Error Codes**

<b>Error Code</b>	<b>Description</b>
101	Unable to load sdf.dll
102	Unable to load addresses to SDF subroutines
103	Unable to find requested lookup table in SDF database
104	Unable to find lookup table for xvalues applied to 1D Table
105	Unable to find lookup table for rvalues applied to 1D Table
106	Unable to find lookup table for xvalues applied to 2D Table
107	Unable to find lookup table for yvalues applied to 2D Table
108	Unable to find lookup table for rvalues applied to 2D Table
109	Unable to find lookup table for xvalues applied to 3D Table
110	Unable to find lookup table for yvalues applied to 3D Table
111	Unable to find lookup table for zvalues applied to 3D Table
112	Unable to find lookup table for rvalues applied to 3D Table
113	Unable to load address to SDF subroutines when called by Preprocessor
114	Invalid value for XFMethod when called by Framework or Preprocessor
115	Missing Simple Data Format DLL: sdf.dll
121	input pipe radius < 0
122	input thickness < 0
123	input thickness >= pipe outer radius
124	input inner crack length < 0
125	input inner crack length >= inner circumference
126	input outer crack length < 0
127	input outer crack length >= outer circumference
128	stype <= 0
129	stype > 6
130	pressure <= 0
131	atmospheric pressure <= 0
132	atmospheric pressure > pressure
133	shape < 1
134	shape > 3
199	input errors - request summary table
215	error in water property calculations

225	error in memory management allocation/deallocation
300	adjusted T0 for 1 degree subcooling
301	applied upper bound Leff_over_Dh=1500
302	recoverable Error: NNES stalled
316	divergence in regular falsi iterations
350	non-recoverable error: no solution found

### 3.2.6 Preprocessing Application

The xLPR Code utilizes the LEAPOR code's development of Use Case 2, a preprocessing application to generate leakage rate tables, in order to reduce computational time. The preprocessing application is used in conjunction with the Excel plug-in, xlpr\_preprocessor.xll. The preprocessing application reads in the required inputs (see Table 8) from the input spreadsheet.

**Table 8. Inputs Read by xLPR LEAPOR Preprocessing Application**

Variable	Unit	Default Value
Pipe Outer Diameter	m	--
Pipe Wall Thickness	m	--
Global Roughness (PWSCC)	mm	113.9*
Local Roughness (PWSCC)	mm	16.86*
Number of Turns (PWSCC)	m <sup>-1</sup>	5940*
Global Path Dev Fact (PWSCC)	--	1.009*
Local Path Dev Fact (PWSCC)	--	1.243*
Global Roughness (Fatigue)	mm	40.51*
Local Roughness (Fatigue)	mm	8.814*
Number of Turns (Fatigue)	m <sup>-1</sup>	6730*
Global Path Dev Fact (Fatigue)	--	1.017*
Local Path Dev Fact (Fatigue)	--	1.06*
Crack Growth Type Choice	--	

\*These default values address requirement SR-LRM-017

If both fatigue and PWSCC, cracking mechanisms are defined as user inputs then the preprocessing application uses the inputs in Table 8 to generate eight leakage rate tables based on the minimum and maximum pressure and temperature values shown in Table 9 using hardcoded values for the crack length and COD discretization (SR-LRM-016). The pressure and temperature values were based on information about the minimum and maximum operating pressures and temperatures of U.S. Nuclear plants.. The determination of these values addresses requirement SR-LRM-015.

**Table 9. Minimum and Maximum Pressure and Temperature for Leakage Rate Tables**

	<b>Pressure (MPa)</b>	<b>Temperature (°C)</b>
Minimum	14.824	280
Maximum	15.913	340

The eight leakage rate tables that are created are:

1. PWSCC Max Pressure Max Temperature,
2. PWSCC Max Pressure Min Temperature,
3. PWSCC Min Pressure Max Temperature,
4. PWSCC Min Pressure Min Temperature,
5. Fatigue Max Pressure Max Temperature,
6. Fatigue Max Pressure Min Temperature,
7. Fatigue Min Pressure Max Temperature, and
8. Fatigue Min Pressure Min Temperature.

If only PWSCC crack growth is considered then only Leak Rate Tables (1)-(4) will be created. If only fatigue crack growth is considered then only Leak Rate Tables (5)-(8) will be created. This method addresses requirement SR-LRM-014. If both fatigue and PWSCC crack growth mechanisms are active in a given xLPR run then the PWSCC leakage rate tables will be used since PWSCC crack growth is faster [50] and therefore more likely to lead to failure. This recommendation addresses requirement SR-LRM-019.

**3.2.6.1 SR-LRM-018 – For the preprocessing application (Use Case 2) provide guidance on how to apply a correction in cases in which the crack opening area differs on the inner and outer diameter.**

The correction method was developed as described in the Leak Rate Module SDD [48] and Section 2.8.1. The correction is only applied when the flow is in Regime 1. When the flow is in Regimes 2, 3, or 4, the deviation from the leak rate value found in the leakage rate tables using the inner diameter crack length and COD (when COA\_inner = COA\_outer) is insignificant and can be ignored. Therefore when the flow is in Regimes 2, 3 or 4 no correction is applied. When the flow is in Regime 1, two leakage rates are pulled from the leak rate table, one using the inner diameter crack length and COD and the other using the outer diameter crack length and COD. These two leakage rates are then averaged to get the corrected leakage rate.

A flow chart that shows the implementation of this correction visually is shown in Section 3.5.

### 3.2.6.2 SR-LRM-020 – Provide guidance on application of the uncertainty due to crack morphology parameters.

The uncertainty due to crack morphology parameters is described in the Leak Rate SDD [48] and Section 2.9. The uncertainty is accounted for by determining the standard deviation of the leakage rate,  $\lambda$ , by interpolating between the 280°C (Equation 24) and 340°C (Equation 25) equations when the leak rate is less than or equal to 4 gpm. Between 4 gpm and 10 gpm a linear fit between the COV value at 4 gpm and the COV value at 10 gpm is used to determine the COV value at the desired leak rate.

Section 3.5 shows the implementation of the uncertainty visually in a flow chart with greater detail provided in the Framework SDD [47].

## 3.3 Description of Inputs

### 3.3.1 LEAPOR USE Case 2 (preprocessing mode) inputs

The xLPR Version 2 Code utilizes LEAPOR's USE Case 2, or preprocessing mode. The inputs for this mode are described in Table 1 of Section 2.2. The inputs Pressure\_max, Pressure\_min, Temperature\_max and Temperature\_min are set to the default values listed in Table 1. The values for these parameters cover the range of interest for the xLPR Version 2 Code. The increment size for the crack length and COD, Ninc\_2c and Ninc\_cod, cannot be changed by the user. Currently this is to ensure both adequate spacing for accuracy and computational efficiency. The crack morphology parameter inputs are for two degradation types: PWSCC and fatigue. The recommended, default values are shown in Table 1 and in Table 10. Table 10 also shows the standard deviation for each crack morphology variable. It is recommended that users stay within one standard deviation if they choose to change the default value.

**Table 10. Crack Morphology mean and standard deviation values**

Crack Morphology Variable	Fatigue		PWSCC	
	Mean	Standard Deviation	Mean	Standard Deviation
$\mu_L$ , $\mu\text{m}$	8.814	2.972	16.86	13.57
$\mu_G$ , $\mu\text{m}$	40.51	17.65	113.9	90.97
$n_{tL}$ , $\text{mm}^{-1}$	6.730	8.070	5.940	4.540
$K_G$	1.017	0.0163	1.009	0.011
$K_{G+L}$	1.060	0.0300	1.243	0.079

### 3.3.2 Leak Rate module runtime inputs

During runtime the Framework is required to perform several calculations or procedure in the process of determining the final leakage rate. These include:

- Determine the appropriate leak rate table(s) to use for a set of given inputs
- Interpolate between tables and/or crack length and COD inputs to determine the leakage rate for a set of given inputs

- Calculate the hydraulic diameter
- Calculate the thickness to hydraulic diameter ratio
- Calculate the inner diameter crack-opening area to outer diameter crack-opening area ratio
- Determine the applicable correction
- Determine the uncertainty factor and interpolate as necessary

In order to perform the above calculations or procedure the Framework needs additional inputs. These inputs are described in Table 3. The inner diameter crack size parameters are used to determine the leakage rate from the leak rate tables. The STYPE variable, temperature and pressure are used to determine the appropriate leak rate table, and the outer diameter crack size variables are used to determine the leakage rate from the leak rate tables if the inner and outer crack opening areas are different and flow is in Regime 1.

### **3.4 Module Verification and Validation**

This section provides a brief summary of the verification and validation efforts that took place for the Leak Rate Module. Full details for the test cases can be found in the Leak Rate Module STP [52], STRR [53] and MVR [45]. The Leak Rate Module Verification and Validation is divided into five main subsections: unit test verification which verifies the technical components of the software code, database verification which ensures the preprocessing use case is developing the leak rate tables correctly, software verification which checks that LEAPOR is calculating leakage rates similar to other leakage rate software codes, in this case SQUIRT, and experimental validation which compares the leakage rates calculated by LEAPOR with available experimental data.

#### **3.4.1 Unit Test Verification**

The unit tests are simply ensuring that the internal functions and solvers of the software code are operating as they should. Therefore, the inputs are internal and unchanged by the user input parameters. The results of the unit tests are shown in Figure 11. As this figure shows, the functions and solvers of the software code are performing as they should.

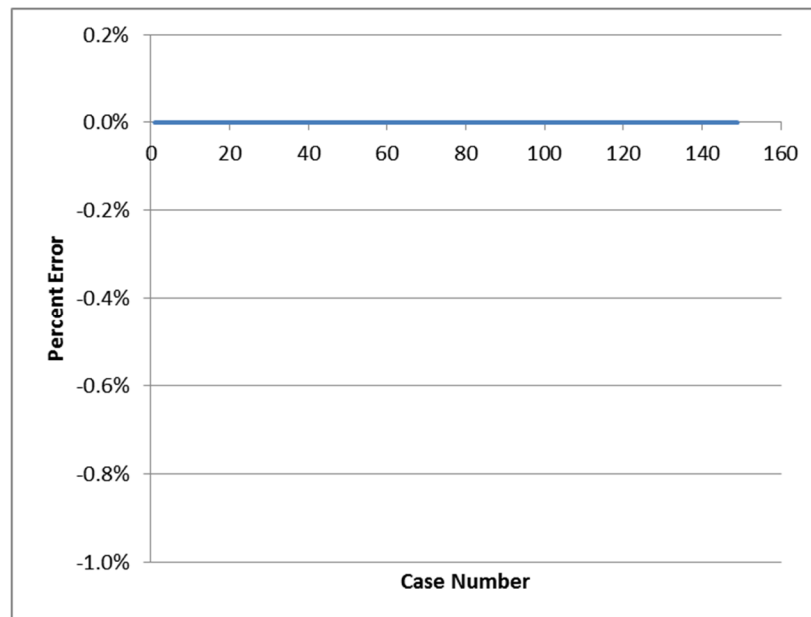


**Figure 11. Unit Test Percent Error of Calculated vs Expected Result (Percent Error vs Case Number)**

The components of the LEAPOR code that are tested include the steam tables, thermohydraulic properties, crack geometry class, error logging and the NNES iteration scheme. The unit test output shown in tabular form can be found in Attachment D of the Leak Rate STRR [53].

### 3.4.2 Database Verification

In order to test that the database is correctly being generated, the Database Inspection Utility is utilized. The Database Inspection Utility reads the database file generated by LEAPOR and graphically shows the result. These results can then be exported to a Comma-Separated Values (csv) formatted text file. The expected result of the visual representation is continuous curves for each crack length. The results from the Database Inspection Utility are shown in Figure 12.

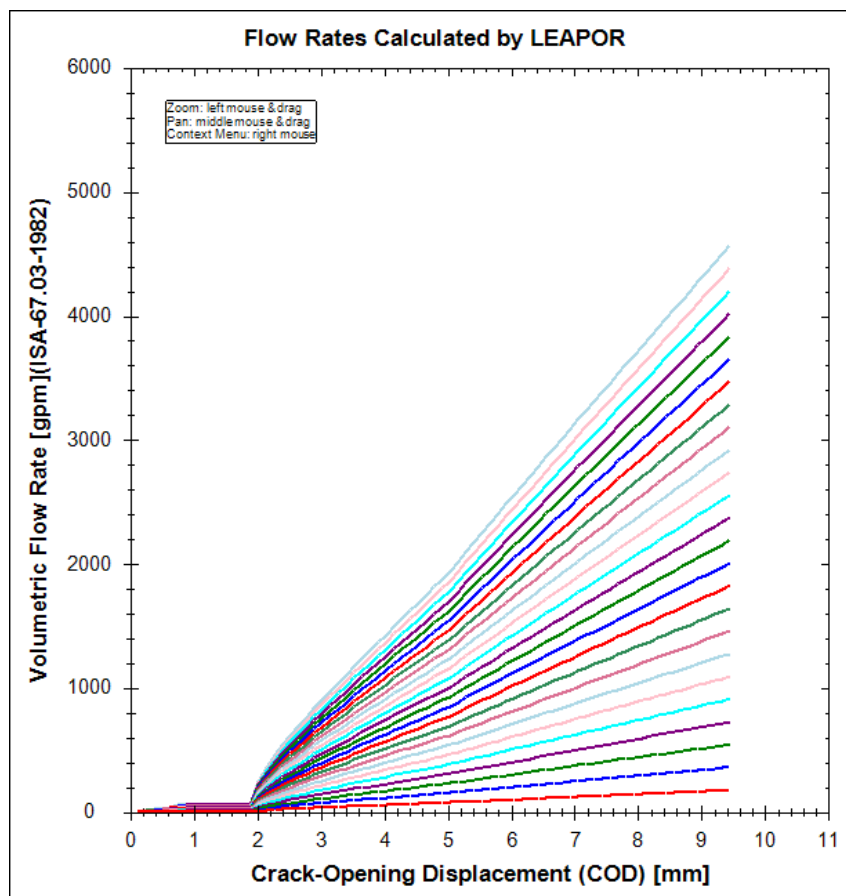


**Figure 12. Database Inspection Utility Results**

As this figure shows, there are no anomalies seen since the shape is expected (see Figure 6) and there are no discontinuities, indicating that the database is being created as it is intended. Other graphical views of the database are shown in Attachment F of the Leak Rate STRR [53].

### 3.4.3 Software Verification

SQUIRT, which stands for Seepage Quantification of Upsets in Reactor Tubes, is a leak-rate computer code originally developed as part of the First International Piping Integrity Research Group (IPIRG) program [30]. The SQUIRT code was initially intended to handle leakage of subcooled water through a crack, where the subcooled water flashes to steam along the crack path. Additionally, the analysis was limited to critical flow at the exit plane of the crack, where the fluid flow was limited by its sonic velocity. The two-phase flow model in SQUIRT is based on the same two-phase flow model through long channels first proposed by Henry and Fauske [16, 17, 18] that is implemented in LEAPOR and described in Section 2.4 and the Leak Rate Module SDD

[48]. As stated previously, this model is considered valid when the ratio of the crack depth to the hydraulic diameter is greater than 15, and an orifice flow model can be used when this ratio is less than 0.5. However, when this ratio is between 0.5 and 15, and the flow is in the transitional two-phase flow region, SQUIRT does not have a model to handle such cases (see Figure 4). This is the major limitation associated with SQUIRT. When the conditions exist such that the flow is in this transitional flow regime, then the code provides suitable warning messages to alert the user to the problem at hand. Although the two codes are based on the same thermohydraulic model, LEAPOR has several improvements to SQUIRT.

Since both SQUIRT and LEAPOR use the same thermohydraulic model, both software codes were validated with the same experimental data described in Section 3.4.4. The results from the SQUIRT runs in comparison to the LEAPOR runs for the artificial crack experimental data are shown graphically in Figure 13. As that figure shows, there are 4 cases in which the results between LEAPOR and SQUIRT differ by more than 10%. The first case (~90% error) is a high pressure/high temperature case in which the flow regime is very close to the transition flow regime. Since the LEAPOR prediction is closer to the measured value than the SQUIRT prediction, it is determined that this error results from the Henry-Fauske model not being valid in the transition flow regime. For the second case (~-70% error), this is the only experimental case data in which the flow was in Regime 4, or orifice flow. In SQUIRT, it is better to use the single phase flow option to calculate the flow rate for orifice flow rather than the subcooled flow option; however the input was not defined that way for the SQUIRT run. Additionally, the orifice flow model was improved in LEAPOR which accounts for the discrepancy. Finally, the third and fourth cases (~41% and ~22% error) may just simply be a rounding error. Although this seems to be a significant error for simply round-off, the SQUIRT code was created with the assumption that the flow rate unit of interest would be gallons per minute (gpm) or liters per min, and therefore when outputting the leakage rate in units of kilograms per second only two digits following the decimal were used. For these particular cases, the SQUIRT output was 0.02 kg/s and 0.01 kg/s and the LEAPOR output was 0.015525 kg/s and 0.005807 kg/s. If the LEAPOR output were to be rounded to two places after the decimal, it would also be 0.02 kg/s and 0.01 kg/s respectively.

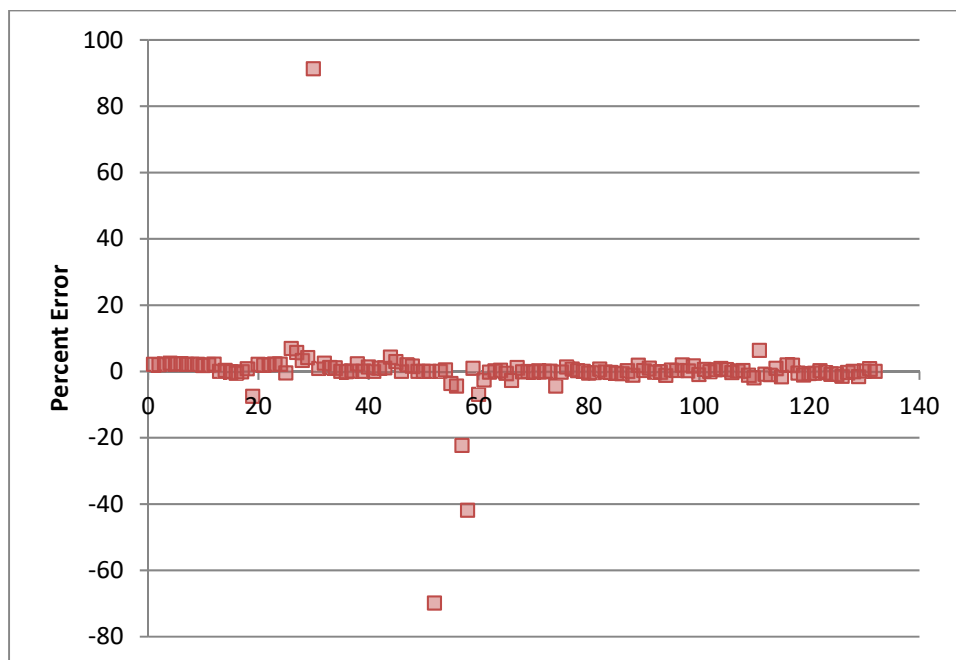


**Figure 13. Percent Error between LEAPOR and SQUIRT runs**



### 3.4.4 Experimental Validation

LEAPOR was validated against the available laboratory data divided into three categories: pipe flows, flows through artificially produced slits, and flows through naturally occurring pipe cracks. The data used in the experimental validation exercise were also used in the original validation of the SQUIRT software code. SQUIRT was implemented into xLPR Version 1.0 and its physical models provide the basis for the Leakage Rate Module. Therefore these experimental data sets offer a useful benchmark in comparing leakage rate calculations in xLPR Version 2.0 with xLPR Version 1.0. The Henry-Fauske model on which LEAPOR is based uses the assumption that fluid is flowing through a long pipe. The fluid path as it flows through a crack can be approximated by a long elliptical-shaped cylinder. The modifications to the Henry-Fauske model attempt to better replicate the effects on the fluid flow by the actual crack shape. LEAPOR has the option to use a rectangular, elliptical or diamond shaped cross section for calculating the leakage rate. The data of Sozzi and Sutherland [39] is flow through a horizontal pipe with no roughness or crack morphology parameters and is used to validate the basic Henry-Fauske model. The data from Collier, et al. [10], Amos and Schrock [2] and Yano [54] represent flow through artificial slits where LEAPOR uses a rectangular shaped cross section and no crack morphology parameters other than the global roughness, are defined. The pipe data from Collier [10] represents flow through a crack, and LEAPOR uses an elliptical cross section and the default crack morphology parameters. The default crack morphology parameters are based on limited data and the uncertainty associated with these parameters is significant. Therefore it is expected to see the most deviation in LEAPOR calculations to experimental measurements for these data sets.

The results from the LEAPOR predictions are compared to all experimental data sets in Figure 14. The majority of the data falls within a reasonable error percentage of less than 20%. Figure 14 also shows the SQUIRT predictions for the same data sets overlaid on the LEAPOR results. As this figure shows the LEAPOR predictions for the experimental data are close to (within 5%) or better than the SQUIRT predictions for almost all cases.

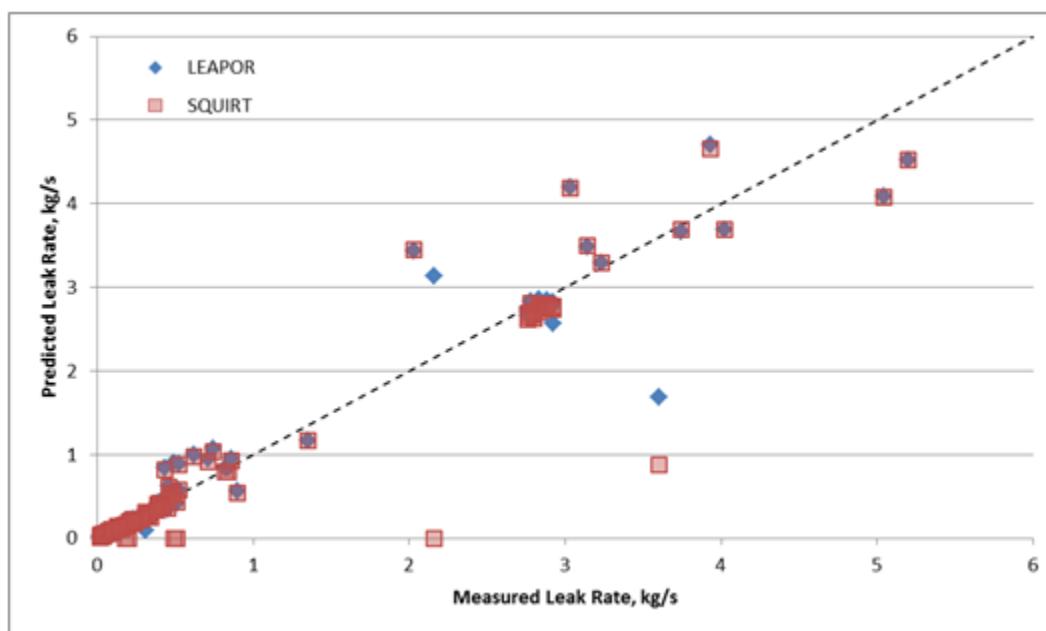
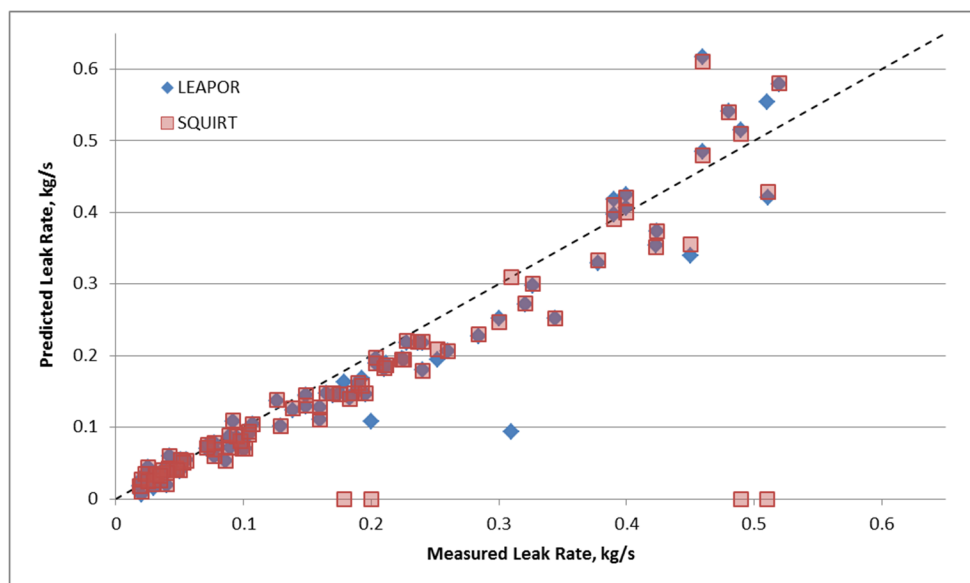


Figure 14. LEAPOR and SQUIRT predicted versus measured leak rates



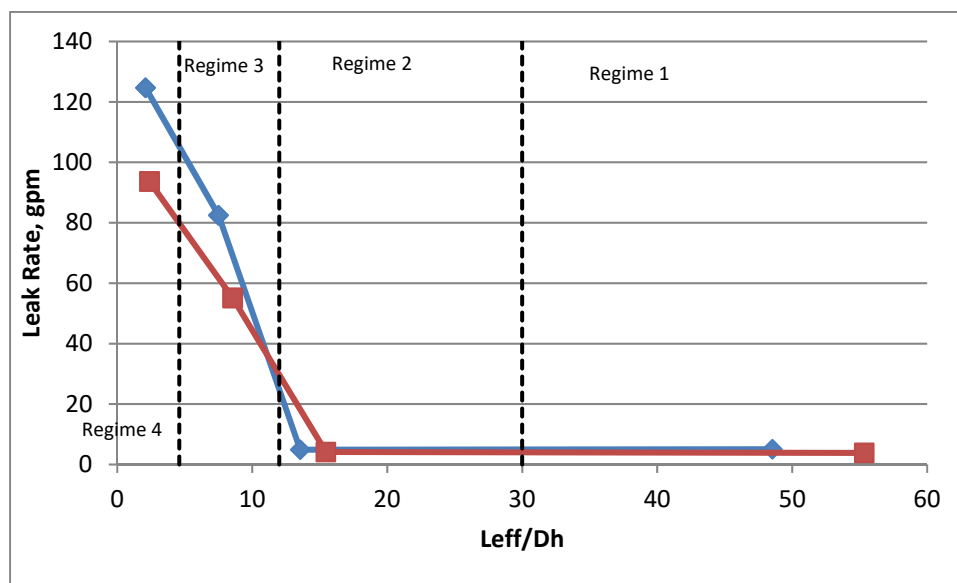
**Figure 15. All Experimental Data up to 10 gpm (approximately 0.63 kg/s)**

Figure 15 shows the experimental measurements versus LEAPOR and SQUIRT predictions for leak rates up to approximately 0.63 kg/s, which corresponds to 10 gpm. This is the region of highest interest for leakage rates since it is the ten times safety factor on the leakage detection capability. As can be seen in Figure 15 the data falls on the 1:1 line without any bias.

In summary, all of the LEAPOR analyses show good agreement with the experimental data through artificial slits with an average error percentage of 18%. Even the Collier pipe data which represents cracks in pipes where some of the crack morphology parameters are utilized shows reasonable predictions with an average of 37% error. These results show good confidence in the use of the Henry-Fauske thermohydraulic model. There is clearly uncertainty in the crack morphology parameters since the percent error increases when compared to the Collier pipe data. However, these results also show good confidence in the use of the crack morphology variables as they are currently defined given the lack of bias in the LEAPOR calculations compared to the Collier pipe data. These results are discussed in much greater detail in the Leak Rate Module MVR [45] including comparisons to each experimental data set.

### 3.4.5 Engineering Judgement Validation

One major improvement written into the LEAPOR code is a transition flow regime model. This model bridges the gap in known solutions between orifice flow and tight cracks (see Figure 4). Since the SQUIRT code does not have this capability there is currently no software code or experimental data to validate the results for test cases that fall into this regime. Therefore, test cases were created that vary the crack length and COD values to ensure the flow will fall into each of the 4 regimes as described below. Since the transition flow model is a smooth transition from Regime 2 to Regime 4, the model is validated by plotting the leakage rate as a function of  $L/D_h$ . A successful test would show a smooth transition from Regime 1 to Regime 4 while an anomalous event would not.

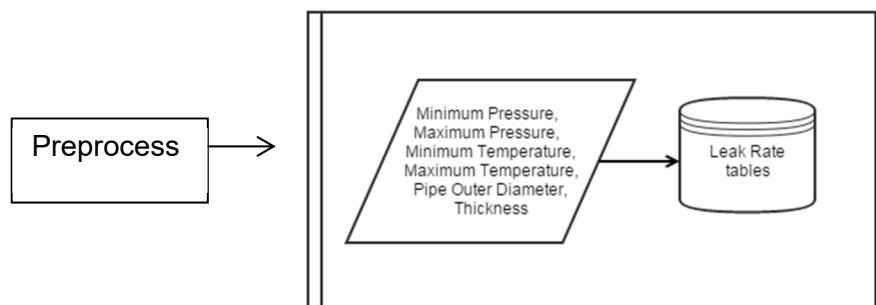


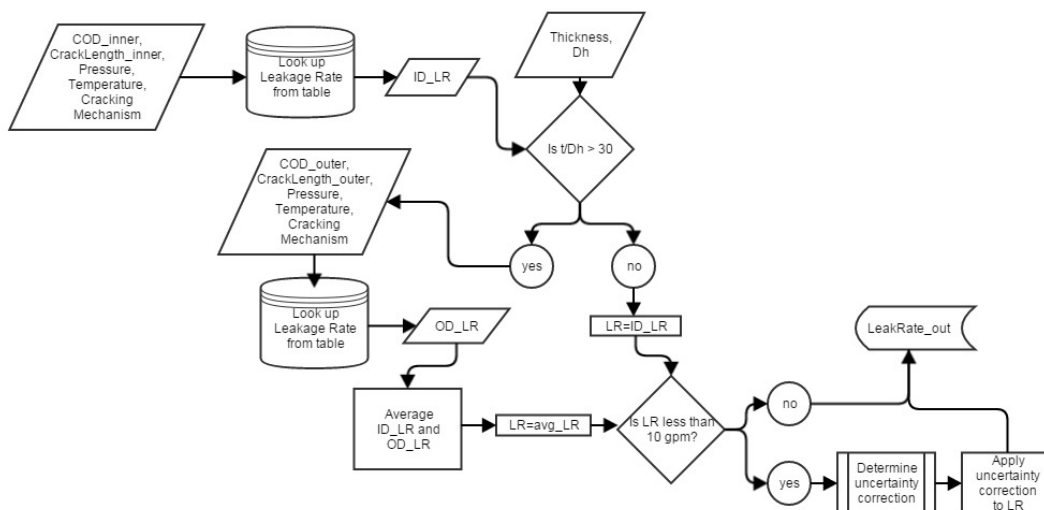
**Figure 16. Calculated Leak Rates for two different COD values over all four regimes**

As Figure 16 shows there is a smooth transition from Regime 2 to Regime 4. Since we have no experimental data by which to compare the results in Regime 3 (the transition flow regime), and under the assumptions for the development of Regime 3 outlined in the SRD[51] and SDD[48], the smooth transition shows that the results of the leakage rate calculation within this regime are as expected and therefore valid.

### 3.5 Flow Diagram

The diagram below shows the logic and implementation of the Leak Rate Module for determining the leakage rate calculated by the xLPR Code.





## **4. RECOMMENDATIONS FOR XLPR VERSION 3 MODIFICATIONS**

There are two variables that have relationships that currently have no technical basis that has been determined. The Darcy friction factor,  $f$ , equation (Equation 11) contains two coefficients,  $C_1$  and  $C_2$  whose values were taken from SQUIRT source code, however the documentation of these values is not found. The velocity head loss,  $e_{vloss}$ , equation (Equation 14) presents a relationship between the effective flow path length and the number of turns crack morphology variable. This relationship was also taken from the SQUIRT source code but its documentation cannot be found. Therefore it is recommended that validation of the Darcy friction factor coefficients and the velocity head loss equation are performed.

Currently in xLPR Version 2.0 there are up to two corrections applied to the leakage rate. The first correction is for the case when the flow is in Regime 1. This correction is necessary due to the fact that leak rate tables are utilized in which the assumption of the same area on the inner and outer diameter is necessary for development and this assumption is almost never true in reality. The correction method approximates the actual leak rate by using the average of the leakage rates calculated by using the inner diameter crack size and the outer diameter crack size. If the leakage rate could be calculated during runtime rather than in the preprocessing stage without significantly increasing the computational time to run the xLPR code then this method would be recommended to improve the accuracy of the calculated leakage rate. The second correction factor is due to the uncertainty of the crack morphology variables. While this correction will always be necessary the degree of uncertainty in the crack morphology variables could be improved. Currently the mean value of each of the crack morphology variables is based on limited data and the standard deviations are very high. By collecting more data and performing more measurements these values could be refined.

In the development of the leak rate tables, currently the minimum and maximum pressure and temperature values are input by the user from the USER\_OPTIONS worksheet (located in the Inputs Database). If a problem is run where the pressure or temperature falls outside that range, the accuracy of the calculated leakage rate cannot be guaranteed. It is recommended that this restriction be lifted in future xLPR Versions. Lifting this restriction would also require the correction method for different inner and outer diameter COAs and uncertainty factors to potentially be redeveloped. The other values that are currently hard-coded are the incrementation size of the crack length and cod in the leak rate table development. It is recommended that those are NOT changeable by the user. If the user were to make these parameters very small the computational time would increase significantly, as would the storage space required, but the increase in accuracy would be negligible. Investigating whether these parameters can be optimized within either LEAPOR or the xLPR preprocessing application and be problem-specific would be recommended.

## **5. LESSONS-LEARNED**

The major lesson learned is the importance of the crack morphology variables in accurately calculating the leakage rate. Using the LEAPOR code to generate leak rate tables in the preprocessing stage has forced the investigation of how the leakage rate changes when assuming an ideal crack shape rather than using the actual values on the inner and outer diameter. It was discovered that the inner diameter crack shape is more important in determining the leakage rate when the fluid flow is in Regimes 2, 3 or 4. When the flow is in Regime 1, which is the Regime that corresponds to the Henry-Fauske flow, transitioning cracks, smaller leak rates and where the crack morphology has the biggest effect, using an average of the leakage rates calculated using the inner diameter properties and the outer diameter properties provides a good approximation for the cases that were examined.

In doing the uncertainty analysis, it was previously assumed that the relationships between the crack morphology variables and the leakage rate would be normally distributed but this was discovered not to be the case. This is likely due in large part to the limited amount of data available. Since the distributions are not standard distributions it shows that obtaining more crack morphology measurements is very important in improving the confidence of the crack morphology model. The only other parameter in the leakage rate equations that is empirically based is the discharge coefficient. It was discovered during analyses that the greatest deviation from the leakage rate that could occur by changing the value of this parameter is less than 2%. This also underscores that the crack morphology uncertainty dominates the uncertainty of any other aspect of the leak rate model.

## **6. SUMMARY**

This Model subgroup report has described the development and implementation of a module to calculate the leakage rate through a crack in nuclear application. A major accomplishment of the Leak Rate subgroup is the development of LEAPOR by ORNL as a software tool that is capable of calculating leakage rates through cracks over all flow regimes of interest and meets the quality assurance standards of the xLPR program. An overview of the leak rate model requirements, selection and development, and uncertainties were presented in Section 2 whereas the implementation of these requirements was presented in Section 3. Section 4 provides recommendations for modifications to the leak rate module in future versions of xLPR and Section 5 outlines the lessons learned. More detailed descriptions of the models selected and the module development are found in the Leak Rate module SRD [51], SDD [48], STP [52], STRR [53], and MVR [45].

## 7. REFERENCES

1. D. Abdollahian, "Calculation of Leak Rates Through Cracks in Pipes and Tubes," EPRI Report NP-3395, 1983.
2. Amos, C. and Schrock, V., "Critical Discharge of Initially Subcooled Water Through Slits," NUREG/CR-3475 (1983).
3. R. S. Bain, *Nonmonotonic Nonlinear Equation Solver (NNES) User's Manual*, Leeds University, Leeds, UK, 1993.
4. S.K. Bandyopadhyay, et al., "Estimation and Measurement of Leak Flow Through Slits/Pre-Cracked Pipes," *BARC News Letter*, Issue No. 281, June 2007.
5. H.S. Bean, ed., *Fluid Meters: Their Theory and Applications*, 6<sup>th</sup> ed., American Society of Mechanical Engineers, New York, 1971.
6. R. D. Blevins, *Applied Fluid Dynamics Handbook*, Van Nostrand Reinhold Co., Inc, New York, 1984.
7. S. J. Chapman, *Fortran 95/2003 for Scientists and Engineers*, 3<sup>rd</sup> ed., McGraw-Hill, New York, NY, 2008.
8. B. Chexal, "Analytical Prediction of Single-Phase and Two-Phase Flow Through Cracks in Pipes and Tubes," *Proc. Heat Transfer – Niagara Falls – AIChE Symposium Series* 80(236), (1984) 19-23.
9. N. S. Clerman and W. Spector, *Modern Fortran – Style and Usage*, Cambridge University Press, Cambridge, UK, 2012.
10. Collier, R. P., Stulen, F. B., Mayfield, M. E., Pape, D. B., and Scott P. M., "Two-Phase Flow Through Intergranular Stress Corrosion Cracks and Resulting Acoustic Emission," EPRI Report No. NP-3540-LD, (1984).
11. E. Elias and G.S. Lellouche, "Two-Phase Critical Flow," *International Journal of Multiphase Flow* 28, (2002) 21-50.
12. B. Fornberg, "Generation of Finite Difference Formulas on Arbitrarily Spaced Grids," *Mathematics of Computation* 51(44), (1988) 699-706.
13. *GoldSim User's Guide, Probabilistic Simulation Environment, Vol.1*, GoldSim Technology Group, Version 10.5, December 2010.
14. N.D. Ghadiali, G.M. Wilkowski, S. Rahman. Summary Report: Effect of Crack Morphology on Leak Rates (Coefficient of Variation), Battelle Memorial Institute report to SAQ Kontroll AB, Bjorn Brickstad, Stockholm Sweden
15. B. Ghosh, et al., "Leak Rates Through Cracks and Slits in PHT Pipes for LBB," *Nuclear Engineering and Design* 212, (2002) 85-97.
16. R. Henry, "The Two-Phase Critical Discharge of Initially Saturated or Subcooled Liquid," *Nuclear Science and Engineering* 41, (1970) 336-342.
17. R.E. Henry, H.K. Fauske, and S.T. McComas, "Two-Phase Critical Flow at Low Qualities, Part I: Experimental," *Nuclear Science and Engineering* 41 (1970) 79 91, "Two-Phase Critical Flow at Low Qualities, Part II: Analysis," *Nuclear Science and Engineering* 41 (1970) 92-98.
18. R. E. Henry and H. K. Fauske, "The Two-Phase Critical Flow of One-Component Mixtures in Nozzles, Orifices, and Short Tubes," *Transactions of the ASME Journal of Heat Transfer* 95 (1971) 179-187.
19. IEEE/ASTM SI 10™ 2010, *American National Standard for Metric Practice*.
20. *IEEE Standard for Information Technology – Systems Design – Software Design Descriptions*, IEEE Std 1016-2009, IEEE Computer Society, New York, N.Y., July 20, 2009.
21. *International Standards Organization ISO/IEC 1539-1:2004: Information technology – Programming languages – Fortran – Part 1: Base Language*, (informally known as



- Fortran 2003), International Organization for Standardization, Geneva, Switzerland, 2004.
22. H. John, J. Riemann, F. Westphal, and L. Friedel, "Critical Two-Phase Flow Through Rough Slits," *International Journal of Multiphase Flow* 14(2), (1988) 155-174.
  23. D. S. Kupperman, et al., *Barrier Integrity Research Program – Final Report*, NUREG/CR-6861 (ANL-04/26), Argonne National Laboratory, December 2004.
  24. E. Kurth, "xLPR Leak Rate Group Work Plan," Engineering Mechanics Corporation of Columbus (EMC<sup>2</sup>), Columbus, OH, October 1, 2011.
  25. R. Kurth, E. Kurth, "SQUIRT 3.0 Comparisons to LEAPOR 1.0 and Initial Crack Morphology Uncertainty Assessments," *Internal Report*, August 4<sup>th</sup>, 2013.
  26. C. Larman, *Applying UML and Patterns – An Introduction to Object-Oriented Analysis and Design and Iterative Development*, 3<sup>rd</sup>. ed., Prentice Hall PTR, Upper Saddle River, NJ, USA (2005).
  27. LEAPOR Source Code, "xLPR\_LEAPOR.vfproj" in Subversion directory - `\\xlpri\tags\Source Code\LEAPOR`.
  28. OMG formal/2007-11-02, Unified Modeling Language (OMG UML), Superstructure, version 2.1.2, November 2007.
  29. OMG formal/2007-11-04, Unified Modeling Language (OMG UML), Infrastructure, version 2.1.2, November 2007.
  30. D.D. Paul, et al., *Evaluation and Refinement of Leak-Rate Estimation Models*, NUREG/CR-5128 (BMI-2164), Rev. 1, Battelle, Columbus, OH, April 1994.
  31. D. Paul and A. Cox, "xLPR Model/Module Conceptual Description: SQUIRT, v3.0 (xLPR SQUIRT, v1.0)," July 26, 2010.
  32. PROMETHEUS, "THE THEORY, VERIFICATION AND BENCHMARKING OF PROMETHEUS," December, 2015.
  33. S. Rahman, et al., *Probabilistic Pipe Fracture Evaluations for Leak-Rate-Detection Applications*, NUREG/CR-6004 (BMI-2174), Battelle, Columbus, OH, April 1995.
  34. Regulatory Guide 1.45, Revision 1, "Guidance on Monitoring and Responding to Reactor Coolant System Leakage," U.S. Nuclear Regulatory Commission, Washington, DC, May 2008.
  35. D. Rouson, J. Xia, and X Xu, *Scientific Software Design – The Object Oriented Way*, Cambridge University Press, Cambridge, UK, 2011.
  36. D. Rudland and C. Harrington, *xLPR Pilot Study Report*, NUREG-2110, U.S. Nuclear Regulatory Commission, Rockville, MD, May 2012 (Adams accession no. ML12145A470).
  37. P.M. Scott, et al., *Development of the PRO-LOCA Probabilistic Fracture Mechanics Code, MERIT Final Report*, Report number: 2010:46 ISSN: 2000-0456, Swedish Radiation Safety Authority, December, 2010.
  38. P.M. Scott, et al., "Report for Subtask 1a for Technical Development of Loss of Coolant Accident Frequency Distribution Program, Subtask 1a: Finalize and QA SQUIRT Code," Battelle, Columbus, OH (no date given).
  39. Sozzi, G. L., and Sutherland, W. A. (1975). "Critical Flow of Saturated and Subcooled Water at High Pressure, NEDO-13418.
  40. *SQUIRT User's Manual*, Version 1.1, Battelle, Columbus, OH, March 24, 2003.
  41. *Standard for Light Water Reactor Coolant Pressure Boundary Leak Detection*, ISA-67.03-1982, *Instrument Society of America*, Research Triangle Park, North Carolina, USA, October 1982.
  42. E. Valero and I.E. Parra, "The Role of Thermal Disequilibrium in Critical Two-Phase Flow," *International Journal of Multiphase Flow* 28, (2002) 21-50.

43. G.B. Wallis, "Critical Two-Phase Flow," *International Journal for Multiphase Flow* 6, (1980) 97-112.
44. P.T. Williams, *Recommended Programming Practices and Standards for Developing xLPR Modules Using Fortran*, ORNL-2012/41410, Oak Ridge National Laboratory, Oak Ridge, Tennessee, December 2012.
45. xLPR-MVR-LR V1, *xLPR Module Validation Report for a Leakage Rate Module*, Version 1.0, August 2015.
46. xLPR-SCMP-V2, *xLPR Software Configuration Management Plan*.
47. xLPR-SDD-FW V1, *xLPR Software Design Description for xLPR Framework*, Version 1.0, April 2014.
48. xLPR-SDD-LR V1, *xLPR Software Design Description for a Leakage Rate Module*, Version 2.0, November 2015.
49. xLPR-SQAP-V2, *xLPR Software Quality Assurance Plan*.
50. xLPR-SRD-CGR V3.1, *xLPR Software Requirements Description for PWSCC and Fatigue Crack Growth Module*, Version 3.1, December 2015.
51. xLPR-SRD-LRM V1, *xLPR Software Requirements Description for a Leak Rate Module*, Version 1.0, October 2015.
52. xLPR-STP-LRM V1, *xLPR Software Test Plan for a Leak Rate Module*, Version 1.0, October 2015
53. xLPR-STRR-LRM V1, *xLPR Software Test Results Report for a Leak Rate Module*, Version 1.0, October 2015
54. Yano, T. Matsushima, E., and Okamoto, A., "Experimental Study of Leak Flow Rate Through Artificial Slits," SMIRT-9, Vol. G, pp 287-292, (1987).